Trisubstituted Heteropolytungstates as Soluble Metal Oxide Analogues. 4.[1a-c] The Synthesis and Characterization of Organic Solvent-Soluble $(Bu_4N)_{12}H_4P_4W_{30}Nb_6O_{123}$ and $(Bu_4N)_9P_2W_{15}Nb_3O_{62}$ and Solution Spectroscopic and Other Evidence for the Supported Organometallic Derivatives $(Bu_4N)_7[(C_5Me_5)Rh{\cdot}P_2W_{15}Nb_3O_{62}]$ and $(Bu_4N)_7[(C_6H_6)Ru{\cdot}P_2W_{15}Nb_3O_{62}]$

David J. Edlund, Robert J. Saxton, David K. Lyon, and Richard G. Finke*

Department of Chemistry, University of Oregon, Eugene, Oregon 97403

Received May 17, 1987

The synthesis and characterization of the previously unknown triniobium-substituted Dawson heteropolyanion, $P_2W_{15}Nb_3O_{62}^{9-}$, as its organic solvent-soluble Bu_4N^+ salt, are described. The monomer $P_2W_{15}Nb_3O_{62}^{9-}$ is found to undergo formation of a previously unknown Nb–O–Nb bridged species: $2P_2W_{15}Nb_3O_{62}^{9-} + 2H^+ \rightleftharpoons H_2O + P_4W_{30}Nb_6O_{123}^{16-}$ ($\equiv \{[P_2W_{15}Nb_3O_{61}]_2{-}O\}^{16-}$). The initial synthesis, at pH 4.6, yields the Me_4N^+ salt of this aggregate, $(Me_4N)_{12}H_4P_4W_{30}Nb_6O_{123}$. Metathesis with Bu_4N^+ provides the Bu_4N^+ salt, $(Bu_4N)_{12}H_4P_4W_{30}Nb_6O_{123}$. Cleavage/deprotonation of the latter salt with 6 equiv of Bu_4NOH yields $(Bu_4N)_9P_2W_{15}Nb_3O_{62}$, which has been shown to form covalently attached, polyoxoanion-supported $(C_5Me_5)Rh^{2+}$ and $(C_6H_6)Ru^{2+}$ complexes of C_{3v} symmetry in acetonitrile solution by IR, ^1H NMR, ^{31}P NMR, and ^{183}W NMR spectroscopy, solution molecular weight measurements, and tests with ion-exchange resins.

Introduction

Several years ago we reported the first two members of the $[SiW_9M_3O_{40}]^{7-}$ (M = V^{5+}, Nb^{5+}) series of organic solvent-soluble soluble metal oxide analogues, $(Bu_4N)_4H_3SiW_9V_3O_{40}$[1c] and $(Bu_4N)_7SiW_9Nb_3O_{40}$[1a,e] (Figure 1A). These Keggin anion ($[XM_{12}O_{40}]^{n-}$) derivatives are discrete metal oxide clusters containing layers of close-packed oxygens (Figure 1B). As anticipated based on previous work by Stucky,[2] using $Nb_6O_{19}^{8-}$, and by Klemperer, Day, and co-workers,[3] using $Nb_2W_4O_{19}^{4-}$, the trisubstituted $SiW_9M_3O_{40}^{7-}$ (M = V^{5+}, Nb^{5+}) heteropolyanions were shown to contain sufficient surface oxygen charge density to covalently attach $CpTi^{3+}$ and $(C_5Me_5)Rh^{2+}$, thereby providing the first Keggin anion-supported organometallic complexes and the first V^{5+}-substituted polyoxoanion-κ^3O-supported organometallic complexes.[1a-c]

Moreover, these $SiW_9M_3O_{40}^{7-}$-supported organometallics exhibit, as the thermodynamic product, regiospecific attachment of the organometallic moiety to only one of several types of C_s symmetry surface oxygen sites, for example, as shown in Figure 2. Note that the $CpTi^{3+}$ and $(C_5Me_5)Rh^{2+}$ fragments attach preferentially to a B-type[1a-c] triad of edge-sharing MO_6 (M = Nb^{5+}, V^{5+}) octahedra.

In the case of the smaller $Nb_2W_4O_{19}^{4-}$, however, each of the three possible isomers is observed for $[(C_5Me_5)Rh{\cdot}Nb_2W_4O_{19}]^{2-}$.[3d] For $[(OC)_3Re{\cdot}Nb_2W_4O_{19}]^{3-}$,[3a] each of the three possible isomers is observed in solution and a disordered arrangement is observed in the solid state.

Because B-$P_2W_{15}M_3O_{62}^{9-}$ (M = V^{5+}, Nb^{5+}) would be a C_{3v} symmetry structure capped with a B-type triad of M = Nb or V edge-sharing MO_6 octahedra (Figure 3), we undertook the synthesis and characterization of the previously unknown $P_2W_{15}Nb_3O_{62}^{9-}$ as the organic solvent-soluble tetrabutylammonium $(Bu_4N)^+$ salt. This system should be valuable for comparison to the $SiW_9M_3O_{40}^{7-}$ series, since it contains the B-type support site preferred in $CpTi{\cdot}SiW_9Nb_3O_{40}^{4-}$ and $(C_5Me_5)Rh{\cdot}SiW_9Nb_3O_{40}^{5-}$ (Figure 2). Moreover, $P_2W_{15}Nb_3O_{62}^{9-}$ would be only the third such polyoxoanion system for supporting organometallic species (following the $M_6O_{19}^{n-}$ and $SiW_9M_3O_{40}^{7-}$ systems).[4] Additional goals were to prepare and characterize one or more organometallic derivatives of $P_2W_{15}M_3O_{62}^{9-}$ using $(C_5Me_5)Rh^{2+}$, $CpTi^{3+}$, or $(C_6H_6)Ru^{2+}$ for comparison to the corresponding $SiW_9M_3O_{40}^{7-}$ system and to continue our efforts aimed at developing methods for characterizing polyoxoanions in solutions, thereby reducing the depencence upon the exceedingly valuable but slower, disorder-prone, and sometimes unavailable X-ray diffraction structural studies of polyoxoanions.[3d,5a] Solution spectroscopic methods will, of course, be essential as we pursue our primary goals of developing novel catalytic chemistry of polyoxoanion-supported transition-metal catalysts (or catalyst precursors) and understanding them through (solution) mechanistic studies.[6]

It is important at this point to briefly present and discuss pertinent background information on what has proven

(1) (a) Finke, R. G.; Droege, M. W. *J. Am. Chem. Soc.* **1984**, *106*, 7274. (b) Finke, R. G.; Rapko, B.; Saxton, R. J.; Domaille, P. J. *J. Am. Chem. Soc.* **1986**, *108*, 2947. (c) Finke, R. G.; Rapko, B.; Domaille, P. J. *Organometallics* **1986**, *5*, 175. (d) Finke, R. G.; Green, C. A.; Rapko, B. *Inorg. Synth.* **1989**, *27*, in press. (e) Finke, R. G.; Droege, M. W.; Nomiya, K.; Green, C. A., submitted for publication in *Inorg. Synth.*

(2) (a) Stucky, G. D.; Flynn, C. M. *Inorg. Chem.* **1969**, *8*, 178. (b) *Ibid.* **1969**, *8*, 335.

(3) (a) Besecker, C. J.; Klemperer, W. G. *J. Am. Chem. Soc.* **1980**, *102*, 7598. (b) Day, V. W.; Fredrich, M. F.; Thompson, M. R.; Klemperer, W. G.; Liu, R. S.; Shum, W. *Ibid.* **1981**, *103*, 3597. (c) Besecker, C. J.; Klemperer, W. G.; Day, V. W. *Ibid.* **1982**, *104*, 6158. (d) Besecker, C. J.; Day, V. W.; Klemperer, W. G.; Thompson, M. R. *Ibid.* **1984**, *106*, 4125. (e) Besecker, C. J.; Day, V. W.; Klemperer, W. G.; Thompson, M. R. *Inorg. Chem.* **1985**, *24*, 44. (f) Klemperer, W. G.; Day, V. W. *Science (Washington, D.C.)* **1985**, *228*, 533 and references therein.

(4) (a) We include here $CpTiMo_5O_{18}^{3-}$, as it is a $M_6O_{19}^{n-}$ derivative.[3b] Klemperer and co-workers have also shown that trimetaphosphate, $P_3O_9^{3-}$, will bind organometallics.[4b,c] (b) Besecker, C. J.; Day, V. W.; Klemperer, W. G. *Organometallics* **1985**, *4*, 564. (c) Main, D. J. Ph.D. Dissertation, University of Illinois at Urbana–Champaign, 1987.

(5) (a) Harmalker, S. P.; Leparulo, M. A.; Pope, M. T. *J. Am. Chem. Soc.* **1983**, *105*, 4286. (b) Suslick, K. S.; Cook, J. C.; Rapko, B. R.; Droege, M. W.; Finke, R. G. *Inorg. Chem.* **1986**, *25*, 241.

(6) (a) Edlund, D. J.; Finke, R. G., unpublished results. (b) Edlund, D. J.; Finke, R. G. submitted for publication in *Organometallics*.

0276-7333/88/2307-1692$01.50/0

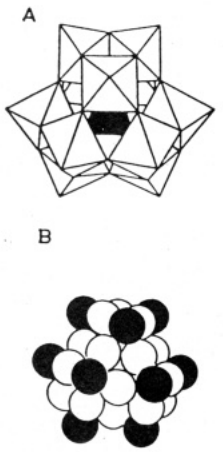

Figure 1. (A) Octahedral and (B) space-filling representations of the Keggin-type heteropolyanion. The open circles in the space-filling model represent bridging oxygens, and the filled (black) circles represent terminal oxygens.

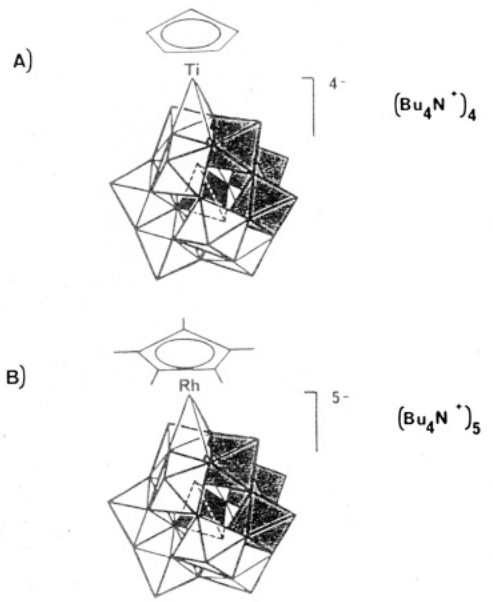

Figure 2. One of the two most plausible C_s symmetry structures for (A) $(Bu_4N)_4[(C_5H_5)Ti{\cdot}SiW_9V_3O_{40}]$ and (B) $(Bu_4N)_5[(C_5Me_5)Rh{\cdot}SiW_9Nb_3O_{40}]$. The other most plausible structure involves bonding of the organometallic moiety to two bridging W–O–M oxygens and a terminal M=O oxygen[25] (M = V, dark octahedra, Figure 2A; M = Nb, dark octahedra, Figure 2B).

to be the most difficult problem in these studies, detecting and thus controlling (via the pH and the amount of water present, for example, vide infra) intermolecular Nb–O–Nb bond formation (anhydride formation) equilibria: 2Nb–OH $\rightleftharpoons$ Nb–O–Nb + H_2O. Recently we presented the first evidence for this process[1a] for A-β-$SiW_9Nb_3O_{40}^{7-}$ which, in the presence of 6 equiv of acid, forms *three* nearly linear Nb–O–Nb bridges via loss of H_2O to provide the C_{3v} symmetry β,β-$Si_2W_{18}Nb_6O_{77}^{8-}$ (eq 1). The structure of β,β-

$$2A\text{-}SiW_9Nb_3O_{40}^{7-} + 6H^+ \rightleftharpoons 3H_2O + Si_2W_{18}Nb_6O_{77}^{8-} \quad (1)$$

$Si_2W_{18}Nb_6O_{77}^{8-}$ is shown in Figure 4. This massive polyoxoanion was isolated as its $6Bu_4N^+$, $2H^+$ salt, $(Bu_4N)_6H_2Si_2W_{18}Nb_6O_{77}$. Five key pieces of data that provide unequivocal evidence for this product are as follows: a fast atom bombardment mass spectrum,[5b] the solution molecular weight via ultracentrifugation, the ^{183}W NMR showing overall C_{3v} symmetry, a characteristic and

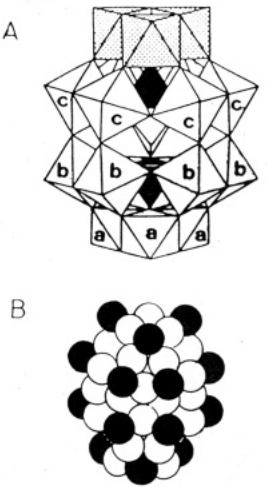

Figure 3. (A) Octahedral and (B) space-filling representations of the Dawson-type heteropolyanion. In B, the open circles in the space-filling model represent bridging oxygens, and the filled circles represent terminal oxygens. In A and for $P_2W_{15}Nb_3O_{62}^{9-}$, the top three (unlabeled) octahedra contain Nb.

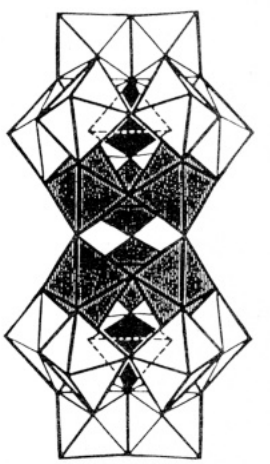

Figure 4. Octahedral representation of the dimer $(Bu_4N)_6H_2Si_2W_{18}Nb_6O_{77}$. The six shaded, central octahedra represent NbO_6 clusters. The three Nb–O–Nb bridging bonds link the two "$SiW_9Nb_3O_{37}^{-}$" halves.

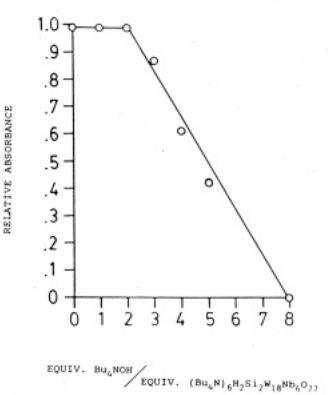

Figure 5. Spectrophotometric titration of $(Bu_4N)_6H_2Si_2W_{18}Nb_6O_{77}$ with aqueous Bu_4NOH. The intensity of the 690 cm^{-1} IR band (attributed to bridging Nb–O–Nb bonds) is plotted as a function of equivalents of added base. The first 2 equiv of Bu_4NOH deprotonate the $H_2Si_2W_{18}Nb_6O_{77}^{6-}$ and therefore do not affect the 690 cm^{-1} band, while the next 6 equiv cleave the three Nb–O–Nb bridging bonds to give 2 $SiW_9Nb_3O_4^{7-}$ + 3 H_2O. Note that zero absorbance has been reached once 8.0 equiv of Bu_4NOH have been added.

intense band in the IR at 690 cm^{-1} due to nearly linear Nb–O–Nb bridging bonds, and a quantitative titration on

Table I. Measured Weight-Average ($\bar{M}_w$) Solution Molecular Weight Values

entry	compound	ν	m	correlatn coeff	calcd MW of anion	obsd $\bar{M}_w$
1	$Li_{9-x}H_xP_2W_{15}Nb_3O_{62}$	0.15	0.287	0.9996	4090	3185
2	$(Bu_4N)_{12}H_4P_4W_{30}Nb_6O_{123}$	0.37	0.313	0.9999	8164	4900[a]
3	$(Bu_4N)_9P_2W_{15}Nb_3O_{62}$	0.46	0.387	0.9991	4090	6270[b]
4	$(Bu_4N)_7[(C_5Me_5)Rh{\cdot}P_2W_{15}Nb_3O_{62}]$	0.37	0.334	0.9972	4328	5380
5	$(Bu_4N)_{12}H_4P_4W_{30}Nb_6O_{123} + H_2SO_4$[c]	0.41	*c*	*c*	8164	*c*

[a] Repeated three times in both reagent grade CH_3CN/0.1 M Bu_4NPF_6 and rigorously dried CH_3CN/0.1 M Bu_4NPF_6 (the latter used in conjunction with flame-dried glassware), average $\bar{M}_w$ = 4900 ± 300. [b] Repeated five times, average $\bar{M}_w$ = 6270 ± 400; this value suggests either ion-paired aggregates or possibly H-bonded (presumably via protons abstracted from water) aggregates.[9e] Two of the ultracentrifugation runs (with material that had apparently decomposed) gave curved rather than linear ln A vs r^2 plots, even though equilibrium had been reached, and are not included in the average $\bar{M}_w$ value. [c] Concentrated H_2SO_4 (15 equiv) was added, and the polyoxoanion concentration was ca. 9×10^{-7} M (optical density 0.3 at 280 nm). See Figure D, supplementary material for the current plot which indicates one species of MW ≥ 11 000.

the 690 cm^{-1} band vs the equivalents of added Bu_4NOH (Figure 5, presented for the first time herein).[7]

The A-type $SiW_9Nb_3O_{40}^{7-}$ structure (consisting of three *corner-sharing* NbO_6 octahedra, Figure 1A) can readily form three nearly linear Nb–O–Nb linkages using the terminal Nb–O bonds (since these are close to being parallel to the C_3 rotational axis centered between the three corner-sharing octahedra). However, inspection of the B-type $P_2W_{15}Nb_3O_{62}^{9-}$ structure (consisting of three adjacent *edge-sharing* NbO_6 octahedra, Figure 3A) makes it apparent that *one* Nb–O–Nb linkage at most appears possible since the terminal Nb–O bonds are closer to being perpendicular to the C_3 rotational axis (between the three edge-sharing octahedra). The single Nb–O–Nb bridged condensation process of interest is shown in eq 2, although

$$2(Bu_4N)_9P_2W_{15}Nb_3O_{62} + 2HX \rightleftharpoons H_2O + (Bu_4N)_{16}P_4W_{18}Nb_6O_{123} \quad (\equiv [Bu_4N]_{16}[(P_2W_{15}Nb_3O_{61})_2{-}O]^{16-}) + 2Bu_4NX \quad (2)$$

at the beginning of this work there was no precedent for such a singly Nb–O–Nb bridged polyoxoanion. Note that such an equilibrium is expected to lie further to the right under acidic conditions or in nonaqueous solvents, but would be shifted toward the left when water or $Bu_4N^+X^-$ is present (conditions found in the ultracentrifugation method for solution molecular weight determinations, for example). One can begin to appreciate the problems in detecting and thus controlling this equilibrium when it is realized that the conditions for ultracentrifugation molecular weight measurement may cause cleavage of the Nb–O–Nb bridge, that the precision of an oxygen analysis (±0.4%, which is ±3 oxygens in this case) cannot distinguish between the monomers and the bridged species, that the $(Bu_4N)_{16}P_4W_{30}Nb_6O_{123}$ has a molecular weight >10 000 (MW = 11 163) so that FAB/MS cannot be used on the Bu_4N^+ salt, that the ^{183}W NMR handle is often lost for protonated polyoxoanions in *dry* organic solvents,[1c] and that the use of X-ray crystallography is virtually ruled out in all but the most favorable cases by the problem of obtaining strongly diffracting, ordered crystals for this size and type of polyoxoanion. (Although we anticipate solving this problem, permutation/combination theory teaches that we are currently searching for the crystalline derivatives *from among 2 042 975 possible combinations* in the case of the 16⁻ species $P_4W_{30}Nb_6O_{123}^{16-}$ and the 25 monocations we are currently investigating.[8a,b]) The problem ultimately reduces, then, to detecting the monomer ⇌ oligomer equilibria, to detecting the Nb–O–Nb bridges

(7) The 690 cm^{-1} IR band, which does not shift with D^+/D_2O treatment and is thereby distinguished from a Nb–OH(D) band, proved to be the crucial handle for detecting dimer formation or cleavage.[1a,16]

(8) (a) Our experience with polyoxoanion crystallizations (of primarily R_4N^+ salts), as well as the literature,[8b] indicates that the greater the charge of the polyoxoanion, the greater the difficulty often in finding a crystalline system (even though there are probably *many* cation combinations that afford crystalline derivatives, vide infra). This is not surprising as shown below using permutation/combination theory, but it appears to be underappreciated.

Since the literature,[8b] as well as our own experience, indicates a *mixture* of countercations is often needed and since the literature shows Na^+, K^+, Rb^+, and Cs^+ salts of polyoxoanions are often recrystallizable from H_2O, we have been investigating, broadly speaking, a range of 25 monocations: Li^+, Na^+, K^+, Rb^+, Cs^+, NH_4^+, $Me_{4-x}NH_x^+$, $Et_{4-x}NH_x^+$, $Pr_{4-x}NH_x^+$, $Bu_{4-x}NH_x^+$ (x = 0–3 in each case), PPN^+, Ph_4As^+, Ph_4P^+ plus some di- and trications as well. The number of possible different combinations, $C(n,x)$, from among n items (25 monocations for example) taken x at a time [e.g. x = 2 for Klemperer's $(C_5Me_5)Rh{\cdot}Nb_2W_4O_{19}^{2-}$ or x = 7 for our $(C_5Me_5)Rh{\cdot}P_2W_{15}Nb_3O_{62}^{7-}$] is given by $C(n,x) = n!/[x!(n-x!)]$ (Bevington, P. R. In *Data Reduction and Error Analysis for the Physical Sciences*; McGraw Hill: New York, 1969; pp 28–30). In the case of the above 2– anion, the number of combinations of 25 monocations is 300 [and crystallography for the $(Bu_4N^+)_2$ salt has been reported[3d]]. In the case of the 4– $CpTi{\cdot}SiW_9V_3O_{40}^{4-}$, 25 cations give 12 650 possible combinations [and the $(Bu_4N^+)_4$ salt is crystalline,[1c] but the examination of many crystals show they diffract poorly; some of the other 12 649 possible cation combinations are under investigation]. For the 7– salt reported herein, $(C_5Me_5)Rh{\cdot}P_2W_{15}Nb_3O_{62}^{7-}$, the number soars to 480 700 [and it has not been crystallized, and it is unlikely it should be as easy to crystallize as $(Bu_4N)_2(C_5Me_5)Rh{\cdot}Nb_2W_4O_{19}$, for example]. For the $P_2W_{15}Nb_3O_{62}^{9-}$ ion, the number of cation combinations (still using 25 different cations) is a whopping 2 042 975 and the number for $P_4W_{30}Nb_6O_{123}^{16-}$ is the same, 2 042 975. Several points are clear. First, it is likely to take some time, or good guesses, to find the crystalline derivatives for highly charged polayanions [although fewer cations via di- or trications, use of fewer (or avoidance) of the less crystalline $R_{4-x}NH_x^+$ cations, and other ideas obvious from the above discussion are being investigated currently]. Secondly, solution spectroscopic (noncrystallographic) methods of characterization such as those used herein are crucial to the development of polyoxoanion chemistry (especially in areas like *catalysis*, where what you *isolate* typically *is not the catalyst*). Thirdly, caution should be used in extrapolating results from less charged systems to seemingly analogous but more highly charged ones [e.g. from $(C_5Me_5)Rh{\cdot}Nb_2W_4O_{19}^{2-}$ to $(C_5Me_5)Rh{\cdot}SiW_9Nb_3O_{40}^{5-}$ or $(C_5Me_5)Rh{\cdot}P_2W_{15}Nb_3O_{62}^{7-}$], either in the solid state or perhaps especially in solution where one can anticipate significant ion-pairing effects yet to be discovered. (b) The polynuclear metal carbonyl (cluster) literature contains evidence of the difficulty in isolation of even 4– or 5– species and suggests the use of multiple or mixed cations. One example is $Pt_{19}(CO)_{22}^{4-}$ where "extensive work involving the use of nine different cations" is reported prior to eventual use of the Bu_4N^+ and Ph_4P^+ salts. (Washechek, D. M.; Wucherer, E. J.; Dahl, L. F.; Ceriotti, A.; Longoni, G.; Manassero, M.; Sansoni, M.; Chiri, P. *J. Am. Chem. Soc.* **1979**, *101*, 6110.) Another example is provided by $Ni_{38}Pt_6(CO)_{48}H^{5-}$. Here the use of the "...combination of spherical $AsPh^{4+}$ and spider-like Bu_4N^+ counterions..." gives rise to crystalline material with good diffraction properties (Ceriotti, A.; Demartin, F.; Longoni, G.; Manassero, M.; Marchionna, M.; Piva, G.; Sansoni, M. *Angew. Chem., Int. Ed. Engl.* **1985**, *24*, 697). (c) ^{17}O NMR is a promising tool for detection of Nb–O–Nb bridged polyoxoanions; Besecker, C. J.; Klemperer, W. G.; Maltbie, D. J.; Wright, D. A. *Inorg. Chem.* **1985**, *24*, 1027. (d) Raman spectroscopy is another promising technique.[8e,6] (e) San Filippo, J., Jr.; Grayson, R. L.; Sniadoch, W. J. *Inorg. Chem.* **1976**, *15*, 269. (f) For related vibrational studies of M–O–M systems see: Hewkin, D. J.; Griffith, W. P. *J. Chem. Soc. A* **1966**, 472; Wing, R. M.; Callahan, K. P. *Inorg. Chem.* **1969**, *8*, 871. (g) For related vibrational studies of polyoxoanions see: Rocchiccioli-Deltcheff, C.; Fournier, M.; Franck, R.; Thouvenot, R. *Inorg. Chem.* **1983**, *22*, 207; **1984**, *23*, 598.

directly,[8] and/or to detecting compositions that differ only in their H^+ and O^{2-} (H_2O) content. Such monomer $\rightleftharpoons$ oligomer equilibria are probably more general in polyoxoanion chemistry than heretofore recognized.[1a,9] Recent findings by Klemperer and co-workers support this view, since single Nb–O–Nb bridge (anhydride) formation, $2\text{-}(Bu_4N)_3HNb_2W_4O_{19} \rightleftharpoons H_2O + (Bu_4N)_6Nb_4W_8O_{37}$, and its reversal by H_2O addition have been observed.[10]

In spite of the above difficulties, we report herein the synthesis and characterization of $(Me_4N)_{12}H_4P_4W_{30}Nb_6O_{123}$, $Li_xH_{9-x}P_2W_{15}Nb_3O_{62}$ in aqueous solution, $(Bu_4N)_{12}H_4P_4W_{30}Nb_6O_{123}$, and its Bu_4NOH cleavage/deprotonation product $(Bu_4N)_9P_2W_{15}Nb_3O_{62}$. We also report solution spectroscopic and other evidence for two supported organometallic derivatives of C_{3v} symmetry, $(Bu_4N)_7[(C_5Me_5)Rh{\cdot}P_2W_{15}Nb_3O_{62}]$ and $(Bu_4N)_7[(C_6H_6)Ru{\cdot}P_2W_{15}Nb_3O_{62}]$. None of these results have been previously reported. Elsewhere we have reported a significantly improved synthesis and characterization of $(Me_4N)_6H_3P_2W_{15}V_3O_{62}$,[1c] $(Bu_4N)_6H_3P_2W_{15}V_3O_{62}$,[1c] $(Bu_4N)_4H_3SiW_9V_3O_{40}$,[1c,d] $(Bu_4N)_6H_2Si_2W_{18}Nb_6O_{77}$,[1e] and $(Bu_4N)_7SiW_9Nb_3O_{40}$[1e] and improved, *Inorganic Syntheses* reports for $(Bu_4N)_4[CpTi{\cdot}SiW_9V_3O_{40}]$[1d] and $(Bu_4N)_3Na_2[(C_5Me_5)Rh{\cdot}SiW_9Nb_3O_{40}]$.[1e]

Experimental Section

Materials. The following were used as received: $Na_2WO_4{\cdot}2H_2O$ Spectrum); 30% H_2O_2 (Fischer); KOH, Na_2CO_3, NaCl, KCl (Baker); $NaHSO_3$, $LiClO_4$ (Mallinckrodt); CD_3CN (Cambridge Isotopes); $RhCl_3{\cdot}3H_2O$, Me_4NCl, Nb_2O_5, Amberlite IRA-400 cation-exchange resin, Amberlyst A-27 anion-exchange resin, 1,8-diazabicyclo[5.4.0]undec-7-ene, and tetrabutylammonium hydroxide as 40% aqueous solution[11] (Aldrich); Bu_4NBr, $NaClO_4$ (Fluka); Celite analytical filter aid (Johns-Manville). Acetonitrile (reagent grade, Baker) was used as received except where dry acetonitrile is noted in the text. Dry acetonitrile was prepared by storing over 3-Å molecular sieve for 5 days prior to use and was then used in flame-dried glassware that was cooled under vacuum.

Instrumentation/Analytical Procedures. Elemental analyses were obtained from Mikroanalytisches Labor Pascher in Bonn, West Germany, unless otherwise noted (because they use the ICP method for metals which yields superior results for polyoxoanions in our experience). Infrared spectra were measured either as KBr pellets, as Nujol mulls, or as acetonitrile solutions in 0.1-mm path-length NaCl cells on a Sargent Welch 3-200 infrared spectrophotometer and referenced to the 1601 cm^{-1} band of polystyrene. Proton and ^{31}P NMR spectra were recorded at 21 °C on a Nicolet NT-360 FT spectrometer at 360.060 and 146.175 MHz, respectively. Proton spectra were referenced to TMS while ^{31}P NMR spectra were referenced to an internal, concentric capillary tube containing 85% H_3PO_4. In each case values upfield of the reference peak are reported as negative values.

^{183}W NMR spectra were recorded at 15.042 MHz by using the same Nicolet instrument, and the spectra were digitized by using 8192 data points with a spectral resolution of 1.2 Hz/data point. The spectrometer was locked on the ^2H resonance of the CD_3CN solvent. Spectra were obtained at 21 °C and referenced to saturated Na_2WO_4/D_2O at 21 °C by using the substitution method. Chemical shifts were calculated in parts per million with negative values reported for resonances upfield of the reference. Spectral parameters for Na_2WO_4/D_2O were as follows: pulse width = 40 μs; acquisition time = 819.4 ms; repetition rate = 2.02 s; sweep width = ±2500 Hz. Spectral parameters for the heteropolyanion sample were as follows: pulse width = 70 μs; acquisition time = 819.4 ms; repetition rate = 821.1 ms; sweep width = ±2500 Hz. In all cases, exponential line broadening of 1 Hz was used.

Weight average ($\bar{M}_w$) solution molecular weights were found by the sedimentation equilibrium method.[12,13] A Beckman Model E ultracentrifuge equipped with a UV optical measurement system was used with a rotation speed of 20000 rpm or 2094.395 rads/min. Heteropolytungstate solutions were prepared by dissolving the sample in either 0.1 M aqueous $LiClO_4$ or 0.1 M Bu_4NPF_6 in acetonitrile and then diluting with the appropriate solvent until an optical density of 0.2–0.4 absorbance units (1-cm path-length cells, ca. 10^{-6} M) was obtained at 250–280 nm depending on the λ_{max} of the sample. With use of double-sectored cells, 25 or more concentration vs distance data points were obtained after equilibrium was reached, typically 12–16 h. In each case the partial molal volume was approximated by the partial specific volume for a 0.005–0.01 M sample concentration and a 0.1 M solution of either Bu_4NPF_6/CH_3CN or $LiClO_4/H_2O$. The specific molar volume was calculated by the method of densities using a 25-mL pyncnometer and an analytical balance (±0.2 mg). The equation used for calculating the molecular weights is a modified Svendberg equation

$$\bar{M}_w = 2RTm/[(1 - \rho\nu)\omega^2] \quad (3)$$

where ν = the partial specific volume, ρ = the solvent density at temperature T, ω = the rotation rate of the ultracentrifuge, and m = the slope of a plot of ln C (or ln A, assuming $A = \epsilon bc$) vs r^2, where r = the distance from the center of the ultracentrifuge rotor to the point where solution concentration (absorbance) is measured.[13a] Table I lists the obtained values and the molecular weights for each of the compounds described in this paper.

We have observed here and in the literature[13b-e] that calculated molecular weights for Bu_4N^+ salts of polyoxoanions in CH_3CN are generally 10–20% higher than the weight of the anhydrous anion even at the dilute ca. 10^{-6} M concentration conditions of the measurement. Equation 3 is an approximation for the case of polyelectrolytes,[13d,e] and, although primary charge effects are suppressed by electrolyte addition, no attempt has been made to account for secondary charge effects or the probability of ion pairing. However, the results obtained herein are clearly sufficient to distinguish monomers from oligomers.

Preparations. $[Rh(C_5Me_5)Cl_2]_2$ was prepared from C_5Me_5H and $RhCl_3{\cdot}3H_2O$ in refluxing solvent according to literature

(9) (a) This finding comes as no surprise, since the mechanism of formation of polyoxoanions is the well-known sequence of protonation, loss of water, and oligomerization until an enclosed structure is formed where the exterior terminal oxygens become polarized toward the interior of the complex[9b,c] resulting in little surface charge density.[9d] (b) Baker, L. C. W. *Advances in the Chemistry of Coordination Compounds*; Kirshner, S., Ed.; MacMillian: New York, 1961; p 609. (c) Baker, L. C. W.; Lebioda, L.; Grochowski, J.; Mukherjee, H. G. *J. Am. Chem. Soc.* **1980**, *102*, 3274; see the discussion on pp 3274–3275 and the caption for Figure 1 therein. (d) Barcza, L.; Pope, M. T. *J. Phys. Chem.* **1973**, *77*, 1795. (e) This is especially true since Day, Klemperer, and Maltbie have recently shown that $H_3V_{10}O_{18}^{3-}$ dimerizes (in non-H-bonding solvents) to $[(H_3V_{10}O_{28})_2]^{6-}$ via six H bonds: Day, V. W.; Klemperer, W. G.; Maltbie, D. J. *J. Am. Chem. Soc.* **1987**, *109*, 2991.

(10) Klemperer, W. G., private communication. We thank Professor Klemperer for sharing this information with us prior to publication.

(11) (a) In our experience, the purity of purchased Bu_4NOH(aq) varies greatly and is usually unacceptable; it is better to prepare aqueous Bu_4NOH directly from Bu_4NX (X = Cl, Br, or I) and Ag_2O.[11b,c] Due to the tendency of Bu_4NOH to degrade by Hofmann elimination, solutions should be refrigerated and periodically checked (by titration to both methyl red and phenophthalein end points) for amine and total base content. (b) Fritz, J. S. *Acid-Base Titrations in Non-Aqueous Solvents*; Allyn & Bacon: Boston, 1973; pp 133–135. (c) Huber, W. *Titrations in Non-Aqueous Solvents*; Academic: New York, 1967; pp 95–100.

(12) (a) Chervenka, C. H. *A Manual of Methods for the Analytical Ultracentrifuge*; Spinco Division of Beckman Instruments, Palo Alto, CA, 1969. (b) Moore, W. J. *Physical Chemistry*; Prentice-Hall: Englewood Cliffs, NJ, 1962; pp 764–772.

(13) (a) A plot of ln C (concentrate of solute) vs r^2 is required by the Svendberg equation. However, it is the slope of this plot that is important. That is, when $A = \epsilon bc$, it follows that $\partial(\ln A)/\partial(r^2) = \partial(\ln C)/\partial(r^2)$ since ϵb is a constant. Therefore, a plot of ln A vs r^2 yields the same slope, hence same calculated molecular weight, as a plot of ln C vs r^2 *if* Beer's law is obeyed. (b) Due either to ion-pairing effects and/or because so-called secondary charge effects[13d] are not accounted for by the modified Svendberg equation, which is an approximation in the case of polyelectrolytes, we and others[13] routinely observe ultracentrifugation molecular weight values for tetrabutylammonium salts of polyoxoanions that are 10–20% high. (c) Sethuraman, P. R.; Leparulo, M. A.; Pope, M. T.; Zonnevijlle, F.; Brevard, C.; Lemerle, J. *J. Am. Chem. Soc.* **1981**, *103*, 7665. (d) Fujita, H. *Foundations of Ultracentrifugal Analysis*; Wiley: New York, 1975; pp 305–313. (e) Eisenberg, H. *Biological Macromolecules and Polyelectrolytes in Solution*; Clarendon: Oxford, 1976; pp 1–62, 100–134.

procedures[1e,14] and its purity checked by ^{1}H NMR (Me_2SO-d_6): δ 1.60 (s, Me).

$K_7HNb_6O_{19}\cdot 13H_2O$ was prepared according to published procedures with slight modifications.[2a,15] Approximately 10 g of Nb_2O_5 (38 mmol) and 20 g of KOH (356 mmol) were fused in a nickel crucible until a uniform and very fluid, colorless liquid was obtained. After the contents were allowed to cool, the solidified mass was removed from the crucible, dissolved in 200 mL of distilled water, and filtered through Celite analytical filter aid. The crude product was precipitated by the addition of an equal volume of 95% ethanol with vigorous stirring, collected, washed with 95% ethanol, and reprecipitated twice more from water with 95% ethanol. The white powder was then dried at 60 °C overnight to yield 16 g (94%). A recent report notes that well-formed crystals of $K_7HNb_6O_{19}\cdot 13H_2O$ can be reproducibly obtained if desired, but only if deionized water is employed and if this water is degassed by boiling vigorously for 15 min immediately prior to use.[15]

α-$K_6P_2W_{18}O_{62}\cdot 14H_2O$ was prepared as previously described by Droege.[16] This synthesis of pure α-$K_6P_2W_{18}O_{62}$ is based on Wu's observation[17] that $P_2W_{17}O_{61}^{10-}$ formed from β-$P_2W_{18}O_{62}$ in the presence of WO_4^{2-} and acid regenerates only α-$P_2W_{18}O_{62}^{6-}$. The mixed-isomer α,β-$K_6P_2W_{18}O_{62}$ was prepared first as follows: 100 g of $Na_2WO_4\cdot 2H_2O$ was dissolved in 350 mL of boiling water. H_3PO_4 (85%, 150 mL) was then added slowly to the boiling solution, and the resulting yellow-green solution was refluxed for 5–10 h. The solution was cooled, and the product was precipitated by the addition of 100 g of KCl. The light green precipitate was collected, dissolved in a minimum of hot water, and allowed to crystallize overnight at 5 °C. Typically, the yield was 70 g after being dried at 80 °C under 0.1–0.3 Torr for several hours. The $K_6P_2W_{18}O_{62}$ prepared in this way is always a mixture of the α and β isomers (ca. 90–95% α isomer) as indicated by NMR: ^{31}P NMR (D_2O) δ (α isomer) −12.6 ± 0.2 and δ (β isomer) −11.0 and −11.6 (±0.2); ^{183}W NMR (D_2O), δ (α isomer) −125.0 and −170.0 (±0.1) and δ (β isomer) −112.0, −131.0, −171.0, and −191.0 (±0.1). The previously described method[1a,16] of base degradation followed by acidification yields the pure α isomer. Approximately 80 g of α,β-$K_6P_2W_{18}O_{62}$ was dissolved in 300 mL of distilled water in a 1500-mL Erlenmeyer flask. To this clear light yellow solution (if the solution is green a drop of bromine can be added to oxidize the heteropolyblue) was added 10% $KHCO_3$ until all the white $K_{10}P_2W_{17}O_{61}$ had precipitated and the supernatant was colorless. Six molar HCl was then added slowly in 5–10 mL portions to regenerate a clear yellow solution of pure α-$K_6P_2W_{18}O_{62}$. The solution was condensed to about 1 L, and then the product was precipitated by addition of 100 g of KCl to the hot solution. After being cooled to 5 °C, the product was collected and recrystallized from hot water to yield 71 g (89%). ^{31}P NMR in D_2O yields a single peak at δ −12.6.

$Na_{12}P_2W_{15}O_{56}\cdot 19H_2O$ (previously formulated[18] by others as "$Na_{12}P_2W_{16}O_{58}$") was prepared according to the following slightly modified procedure.[18] Sodium perchlorate (107 g) was added to an aqueous solution of pure α-$K_6P_2W_{18}O_{62}\cdot 14H_2O$ (75 g in 250 mL of water) and was stirred for 2 h. The insoluble $KClO_4$ was removed by filtration, and 1 M Na_2CO_3 was added to reach pH 9 (roughly 200 mL); the pH was maintained by base addition as required during 1 h of constant stirring. The original light yellow solution turned colorless, and then a white precipitate was formed that was collected on a coarse frit and washed with successive portions of 75 mL of saturated NaCl solution, 75 mL of 95% ethanol, and 75 mL of diethyl ether. The product was then dried overnight at 60 °C. Thermal gravimetric analysis (TGA) indicated 19 waters of hydration. Yield: 60 g (83%). Drying can also be accomplished in a dessicator over concentrated H_2SO_4 for 2 days to yield a $18H_2O$ hydrate (by TGA). Drying over concentrated H_2SO_4 for longer periods of time results in a hygroscopic product. (Note that a report of crystalline $Na_{12}P_2W_{15}O_{56}\cdot xH_2O$ has not appeared and the present literature synthesis probably produces impure material. Purification is possible at the next step, however, vide infra.)

$(Me_4N)_{12}H_4P_4W_{30}Nb_6O_{123}\cdot 16H_2O$. A pale yellow solution was prepared by dissolving 2.95 g of $K_7HNb_6O_{19}\cdot 19H_2O$ (2.15 mmol) in 325 mL of 0.5 M H_2O_2. Next, 29 mL of 1 M HCl was added[19] followed by 18.25 g of $Na_{12}P_2W_{15}O_{56}\cdot 19H_2O$ (4.22 mmol). After complete dissolution of the $Na_{12}P_2W_{15}O_{56}$, $NaHSO_3$ (25 g) was added, resulting in a clear, colorless solution. (Caution! a fume hood must be used at this step.) The resulting solution was stirred 5 min before addition of a large excess (~10 g) of tetramethylammonium chloride. The white precipitate was collected, reprecipitated twice from a homogeneous solution of hot, unbuffered, pH 4.6 water, and dried under vacuum (0.1–0.3 Torr) overnight at 25 °C. Yield: 15.4 g (75%). Several TGAs done on samples prepared throughout the course of these studies showed an average of 16 ± 6 waters of hydration. Anal. Calcd for $C_{48}H_{164}N_{12}P_4W_{30}Nb_6O_{123}\cdot 16H_2O$: C, 6.17; H, 1.77; N, 1.80; P, 1.33; Nb, 5.96; W, 59.00. Found: C, 6.65; H, 1.97; N, 1.86; P, 1.03; Nb, 5.67; W, 59.29; K, 0; Na, 0. IR, ^{31}P and ^{183}W NMR, and other data are provided in the text.

This procedure has been successfully completed more than a dozen times by four different people with satisfactory results each time.

$(Bu_4N)_{12}H_4P_4W_{30}Nb_6O_{123}$. $(Me_4N)_{12}H_4P_4W_{30}Nb_6O_{123}\cdot 16H_2O$ (15 g, 1.60 mmol) was dissolved in hot, pH 4.6 water (500 mL) and filtered over Celite (when necessary) to obtain a clear solution. The solution was then allowed to cool to room temperature. Addition of aqueous tetrabutylammonium bromide (7 g in 20 mL of water) resulted in a rise in pH to 5.8 along with the formation of a white precipitate of the product.[20] The precipitate was collected and washed well with water to remove excess tetrabutylammonium bromide. (The product sometimes precipitates as a very fine powder that readily clogs medium and fine frits. The best results are obtained when solid Bu_4NBr is added to a room temperature solution of the Me_4N^+ salt.) The sample was then dried at 60 °C for 12 h to yield 17.7 g (100%). Material dried in this fashion generally showed ≤1 H_2O by TGA, consistent with our general findings for such Bu_4N^+ salts.[1b] Anal. Calcd for $C_{192}H_{436}N_{12}P_4W_{30}Nb_6O_{123}$: C, 20.82; H, 3.97; N, 1.52; P, 1.12; Nb, 5.03; W, 49.79. Found: (analysis by Galbriath Laboratories): C, 20.50; H, 3.95; N, 1.50; P, 0.99; Nb, 5.16; W, 49.96.

Attempts to crystallize this product were unsuccessful, and reprecipitation from a saturated acetone solution to which a few drops of neutral water had been added, followed by cooling at 5 °C for a few days, provided a fine powder. After being dried at 60 °C for 12 h, this powder was found to be *less pure* by elemental analysis than the original material. Anal. Calcd for $C_{192}H_{436}N_{12}P_4W_{30}Nb_6O_{123}$: C, 20.82; H, 3.97; N, 1.52; P, 1.12; Nb, 5.03; W, 49.79. Found: C, 19.84; H, 3.91; N, 1.50; P, 1.13; Nb, 4.66; W, 50.03.

Crystallization/reprecipitation was also attempted from acetone/pH 2 water, but this yielded decomposition to $P_2W_{18}O_{62}^{6-}$ (^{31}P NMR in CD_3CN; δ −12.7 (α isomer) and δ −11.0 and −11.6 (β isomer)). Minimizing the number of manipulations gave the best material, so that the initial, well-washed, well-dried, and analytically pure product was chosen for subsequent experiments.

$(Bu_4N)_9P_2W_{15}Nb_3O_{62}$. A 3.00-g sample of $(Bu_4N)_{12}H_4P_4W_{30}Nb_6O_{123}$ (0.271 mmol) was dissolved in 10 mL of acetonitrile. To this solution was added 6.0 equiv (1.03 mL) of aqueous Bu_4NOH (40% by weight, 1.57 M) followed by stirring at room temperature for 0.5 h. Solid $(Bu_4N)_9P_2W_{15}Nb_3O_{62}$ was obtained by removal of the solvent under vacuum at 25 °C for 24 h. We have been unable to crystallize $(Bu_4N)_9P_2W_{15}Nb_3O_{62}$ to date, presumably due to the inability of the preferred lattice to accommodate more than six Bu_4N^+ cations.[8a,b,21] However,

(14) Kang, J. W.; Moseley, K.; Maitlis, P. M. *J. Am. Chem. Soc.* **1969**, *91*, 5970.
(15) Filowitz, M.; Ho, R. K. C.; Klemperer, W. G.; Shum, W. *Inorg. Chem.* **1979**, *18*, 93.
(16) Droege, M. W. Ph.D. Dissertation, University of Oregon, 1984.
(17) Wu, J. *Biol. Chem.* **1920**, *43*, 189.
(18) Contant, R.; Ciabrini, P. J. *J. Chem. Res., Synop.* **1977**, *222*; *J. Chem. Res., Miniprint* **1977**, 2601.
(19) Occasionally the yellow solution becomes cloudy within minutes after addition of acid; when this happens, the Nb/H_2O_2 solution is discarded and a fresh solution is prepared. The precipitate is probably $[Nb_2O_5]_n$, most likely a result of insufficient H_2O_2 or impure $K_7HNb_6O_{19}$.
(20) If acid addition (6 M HCl) is employed to maintain the pH at 2 during addition of Bu_4NBr, a highly protonated (>5 equiv of H^+) and CH_3CN-insoluble product is obtained.
(21) See ref 1b, footnote 7, for a discussion of this point.

a microcrystalline product can be obtained if the DBU·H$^+$ (DBU = 1,8-diazabicyclo[5.4.0]undec-7-ene) salt is prepared (vide infra). Purity of the noncrystalline $(Bu_4N)_9P_2W_{15}Nb_3O_{62}$ was ascertained by ^{31}P NMR. All $(Bu_4N)_9P_2W_{15}Nb_3O_{62}$ used in this work exhibited a ^{31}P NMR (CD_3CN) consisting predominantly of the anticipated two lines (δ −7.3 and −14.1 ± 0.2) and two less intense signals at δ −9.1 and −13.8 ± 0.2 (both of <5% relative intensity). These latter two lines are not present in material that has been placed in a 60 °C oven for 24 h. TGA failed to show any solvates in material dried either under vacuum or at 60 °C for 24 h.

Experience with $(Bu_4N)_9P_2W_{15}Nb_3O_{62}$ has shown that it has a short shelf-life, even in the freezer compartment of a refrigerator (perhaps due to H_2O condensation as the cold sample is opened and closed during its use), producing a white, CH_3CN-insoluble material.[22] Therefore, it is suggested that this material be prepared as needed and that prolonged storage (greater than 2 weeks) be avoided. We suspect, but have not proven, that a Hofmann elimination reaction of the Bu_4N^+ cations, $(Bu_4N)_9P_2W_{15}Nb_3O_{62} \rightarrow x Bu_3N + x CH_3CH_2CH{=}CH_2 + (Bu_4N)_{9-x}H_xP_2W_{15}Nb_3O_{62}$, may have occurred and that moisture accelerates the decomposition.

(DBU·H)$_9$P$_2$W$_{15}$Nb$_3$O$_{62}$·11H$_2$O. To a warm (~30 °C) aqueous solution of 5.0 g of $(Me_4N)_{12}H_4P_4W_{30}Nb_6O_{123}\cdot 16H_2O$ (0.535 mmol) was added, with stirring, an excess (2.00 g, 10.6 mmol) of DBU·HCl. Cooling to 0 °C overnight yielded a white precipitate that was collected, washed with 95% ethanol, and then dried at 80 °C under 0.1–0.3 Torr for 3 h to yield 5.3 g. Three grams of this material was then slurried in 100 mL of refluxing CH_3CN/DMSO (5:1), and about 1.5 mL of DBU was added. Refluxing was continued for 17 h, after which time the solution became homogeneous. The volume of the solution was condensed to 25 mL, and addition of 95% ethanol resulted in precipitation of the crude product as a white powder. A microcrystalline product was obtained by slowly cooling a hot, saturated CH_3CN/H_2O (1:1, v/v) solution at 5 °C overnight. Drying at room temperature under 0.1–0.3 Torr for 3 h resulted in 2.50 g (0.441 mmol), 41%. TGA was consistent with 11 waters of hydration. Anal. Calcd for $C_{81}H_{175}N_{18}P_2W_{15}Nb_3O_{73}$: C, 17.17; H, 3.11; N, 4.45; P, 1.09; Nb, 4.92; W, 48.66. Found: C, 16.76; H, 3.15; N, 4.47; P, 1.01; Nb, 4.45; W, 49.49 (analysis by E+R Laboratories). Because the analysis is marginal and because DBU·H$^+$Cl$^-$ is mildly acidic, the product was checked for a 665 cm^{-1} band characteristic of $H_4P_4W_{30}Nb_6O_{123}^{12-}$, but none was found.

(Bu$_4$N)$_7$[(C$_5$Me$_5$)Rh·P$_2$W$_{15}$Nb$_3$O$_{62}$]. Ten milliliters of an acetonitrile solution containing 0.166 g of $[Rh(C_5Me_5)Cl_2]_2$ (0.269 mmol) was added to 0.210 g of $AgBF_4$ (1.08 mmol). A white precipitate formed, and the resultant yellow mixture was stirred for 0.5 h at room temperature. The mixture was filtered and the precipitate washed with 5 mL of acetonitrile. The orange-yellow filtrate and washings were then added dropwise with stirring to a colorless acetonitrile solution containing 3.375 g of $(Bu_4N)_9P_2W_{15}Nb_3O_{62}$ (0.538 mmol). The orange-red solution was refluxed for 1 h. After this time the solvent was removed under vacuum and the solid dried at room temperature and 0.1–0.3 Torr overnight. Repeated attempts to recrystallize the crude product failed, as anticipated, based on our experience with $(Bu_4N)_9P_2W_{15}Nb_3O_{62}$ and the presence of >6 Bu_4N^+ cations[21] in the $(Bu_4N)_7[(C_5Me_5)Rh\cdot P_2W_{15}Nb_3O_{62}]$ product; therefore this product contains 2 equiv of Bu_4NBF_4. However, the clean (C_5Me_5)Rh singlet at 1.92 ± 0.005 ppm in the high S/N (signal/noise) 360-MHz ^1H NMR spectrum indicated only one (>95%) isomer, and only minor impurities were indicated by a high S/N ^{31}P NMR spectrum (Figure 12) while no impurities are observed in the, albeit less sensitive, ^{183}W NMR spectrum (Figure 12), so that this material is fully adequate for the initial solution spectroscopic characterizations reported herein.

Attempts to prepare a crystalline DBU·H$^+$ salt by adding 10 equiv of DBU·HCl to a 0.02 M acetonitrile solution (1 mL) of $(Bu_4N)_7[(C_5Me_5)Rh\cdot P_2W_{15}Nb_3O_{62}]$, followed by cooling at 5 °C overnight and collecting the precipitate, failed as elemental analysis indicated that ~50% of the $C_5Me_5Rh^{2+}$ was cleaved from the polyoxoanion support under these acidic conditions. Further work with other cations is in progress and will be reported in due course.[8a,b]

(Bu$_4$N)$_7$[(C$_6$H$_6$)Ru·P$_2$W$_{15}$Nb$_3$O$_{62}$]. To ten milliliters of an acetonitrile solution containing 0.135 g of $[Ru(C_6H_6)Cl_2]_2$ (0.270 mmol) was added 0.210 g of $AgBF_4$ (1.08 mmol). A white precipitate formed, and the resultant reddish green solution was stirred 0.5 h at room temperature. The mixture was then filtered, and the precipitate was washed with 5 mL of acetonitrile. The reddish green filtrate and washings were then quantitatively transferred dropwise with stirring to a colorless acetonitrile solution containing 3.375 g of $(Bu_4N)_9P_2W_{15}Nb_3O_{62}$ (0.538 mmol). The resultant light red solution was refluxed for 1 h. After this time the solvent was removed under vacuum and the solid product (which contains 2 equiv of Bu_4NBF_4) was dried at room temperature and 0.1–0.3 Torr overnight. ^1H NMR in CD_3CN: $\delta(C_6H_6)$ 5.97 ± 0.005. ^{31}P and ^{183}W NMR, also in CD_3CN, are shown in Figure 14.

Titration of (Bu$_4$N)$_{12}$H$_4$P$_4$W$_{30}$Nb$_6$O$_{123}$ with Bu$_4$NOH. In a typical experiment 1–2 g of $(Bu_4N)_{12}H_4P_4W_{30}Nb_6O_{123}$ was accurately weighed to five significant figures and dissolved in 60 mL of reagent grade DMF. The solution was placed under a dry N_2 atmosphere, at room temperature, and stirred via a magnetic stir bar. Titration data were obtained with a Corning Model 125 pH meter previously calibrated with standard pH 4.01 and 10.00 buffer solutions (Fischer). Data points were obtained in mV. The potential was monitored as a solution of Bu_4NOH in water (1.57 M, 40% by weight) was syringed into the DMF solution in roughly 0.2-equiv intervals. Response to addition of the first 4 equiv of base was rapid, as one would expect for an acid/base titration, but was rather slow during addition of the fifth and sixth equivalents, requiring about 5 min for the pH meter to equilibrate after each aliquot of base was added. The results are given in Figure 10.

Titration of (Bu$_4$N)$_{12}$H$_4$P$_4$W$_{30}$Nb$_6$O$_{123}$ with Bu$_4$NOH by IR. A sample of 0.5 g of $(Bu_4N)_{12}H_4P_4W_{30}Nb_6O_{123}$ was accurately weighed to four significant figures and dissolved in 10 mL of acetonitrile. Aqueous Bu_4NOH (1.57 M, 40% by weight) was added to the sample, at room temperature, in increments of 0.7 equiv. The change in the intensity of the 665, 800, 905, and 955 cm^{-1} bands in the infrared spectrum was recorded (in the absorbance mode) after each successive equivalent and was normalized to the constant absorbance 1090 cm^{-1} band as an internal standard. The sample was stirred for 5 min after addition of each equivalent of base and before the IR spectrum was recorded to ensure complete reaction. The results are given in Figure 8 and Figure A (supplementary materials) and are described in the text. The experiment was repeated three times with identical results within experimental error each time.

Experiments Demonstrating Non-Ion-Exchangeability of Supported Organometallic Cations. A cation-exchange column (7 mm × 270 mm) was packed with Amberlite IRA-400 resin that had been previously washed with aqueous Bu_4NOH until the pH of the wash solution remained strongly basic. Once packed, the column was washed with five 50-mL portions of reagent grade acetonitrile. Roughly 0.1 g of sample (i.e., $[Bu_4N]_7[(C_5Me_5)Rh\cdot P_2W_{15}Nb_3O_{62}]$ or $[Bu_4N]_7[(C_6H_6)Ru\cdot P_2W_{15}Nb_3O_{62}]$) was dissolved in 1 mL of acetonitrile, placed at the top of the resin, and then eluted with acetonitrile at a rate of ca. 1 drop every 10 s.

An anion exchange column of similar proportions was packed with Amberlyst A-27 resin in the Cl$^-$ form and washed with reagent grade acetonitrile. Loading and elution were performed as described above. The results of these experiments are described in the Results and Discussion.

D$_2$O Exchange/IR Studies. In a typical experiment, 0.4959 g of $(Bu_4N)_{12}H_4P_4W_{30}Nb_6O_{123}$ (0.0222 mmol) was dissolved in 10 mL of acetonitrile and the IR spectrum taken of the solution in 0.1-mm path-length NaCl cells using acetonitrile as a reference. Next, 0.2 mL of D_2O (10 mmol) was added to the acetonitrile solution that was then stirred at room temperature for 2 h. After this time the IR spectrum was retaken, using the same NaCl cells, and referenced to a solution of 0.02 mL of D_2O in 1.00 mL of acetonitrile. It revealed no change in position or intensity of the band at 665 cm^{-1} nor in any other band above 600 cm^{-1}. In

(22) One or both of the following characteristics have been observed for $(Bu_4N)_9P_2W_{15}Nb_3O_{62}$ that has been stored, at room temperature, for periods in excess of 2 weeks: the presence of a white, acetonitrile-insoluble fraction or failure to obtain an active olefin hydrogenation catalyst upon hydrogenolysis[6] of coordinated COD from $\{(Bu_4N)_8[(COD)Ir\cdot P_2W_{15}Nb_3O_{62}]\}_x$.

addition, an equivalent amount of the monomer $(Bu_4N)_9P_2W_{15}Nb_3O_{62}$ was cleanly converted to $(Bu_4N)_{12}D_4P_4W_{30}Nb_6O_{123}$ (IR spectrum from 1200 cm^{-1} to 400 cm^{-1}, including the 665 cm^{-1} band, identical with that of authentic material) by stirring in CD_3CN/CD_3COOD solution for 30 min. These experiments were repeated four times with identical results.

Control Experiment on D_2O Exchange/IR Studies. In order to demonstrate that the 665 cm^{-1} band of $(Bu_4N)_{12}H_4P_4W_{30}Nb_6O_{123}$ is surprisingly, but indeed, different from the 660 cm^{-1}, Nb–OH (or Nb–O(H)–Nb), band observed[1a,16] for $(Bu_4N)_{7-x}H_xSiW_9Nb_3O_{40}$ (x = 1 or 2), we did the following side-by-side control experiment. $(Bu_4N)_6H_2Si_2W_{18}Nb_6O_{77}$ (0.4277 g, 0.0647 mmol) was dissolved in 10 mL of acetonitrile. To this solution was added 6.5 equiv of 40% aqueous Bu_4NOH, and the solution was stirred for 30 min. An IR spectrum of this solution, in 0.1-mm path-length NaCl cells referenced to acetonitrile, showed a band at 660 cm^{-1}. After addition of 0.2 mL of D_2O to this solution and stirring for 2 h, the IR spectrum was retaken in the same cells and referenced to a solution of 0.02 mL of D_2O in 1.00 mL of acetonitrile. The 660 cm^{-1} band was no longer evident. After thorough cleaning and drying of the NaCl cells and glassware used in this experiment, this equipment was used to repeat the D_2O shift experiment, using $(Bu_4N)_{12}H_4P_4W_{30}Nb_6O_{123}$, as outlined in the section above. The results were the same as described in the above section. In this case, however, and contrary to the results with the 660 cm^{-1} band of $(Bu_4N)_6H_2Si_2W_{18}Nb_6O_{77}$, the 665 cm^{-1} band of $(Bu_4N)_{12}H_4P_4W_{30}Nb_6O_{123}$ does not shift in position or intensity (see Figure 8 and text for additional discussion).

Results and Discussion

Synthesis of $(Me_4N)_{12}H_4P_4W_{30}Nb_6O_{123}\cdot 16H_2O$, of the Monomeric Aqueous Solution Form $Li_{9-x}H_xP_2W_{15}Nb_3O_{62}$, and of $(Bu_4N)_{12}H_4P_4W_{30}Nb_6O_{123}$. The synthesis of $[H_4P_4W_{30}Nb_6O_{123}]^{12-}$ and of its monomeric, aqueous solution form $[P_2W_{15}Nb_3O_{62}]^{9-}$ was patterned after our successful preparation of $[Si_2W_{18}Nb_6O_{77}]^{8-}$ and its monomeric form $[SiW_9Nb_3O_{40}]^{7-}$.[1a,16] A key step is the use of 0.5 M H_2O_2 to solubilize $[Nb_6O_{19}]^{8-}$ in acidic media. The experimental procedure yields the product on a 15.7-g scale, 75% overall yield (Bu_4N^+ salt), according to the following stoichiometry for formation first of the monomer (eq 4) and then H_2O loss and Nb–O–Nb bridge formation to yield $[H_4P_4W_{30}Nb_6O_{123}]^{12-}$ (eq 5). The evidence for the

$$[Nb_6O_{19}]^{8-} + 2[B\text{-}P_2W_{15}O_{56}]^{12-} + 20H^+ \xrightarrow[2.\ NaHSO_3]{1.\ 0.5\ M\ aqueous\ H_2O_2} 2[H_3P_2W_{15}Nb_3O_{62}]^{6-} + 7\ H_2O \quad (4)$$

$$2[H_3P_2W_{15}Nb_3O_{62}]^{6-} \rightleftharpoons H_2O + [H_4P_4W_{30}Nb_6O_{123}]^{12-} \quad (5)$$

latter process will be presented later in the paper. The resultant $[H_4P_4W_{30}Nb_6O_{123}]^{12-}$ can be precipitated and characterized either as the tetramethylammonium (Me_4N^+) salt or as the tetrabutylammonium (Bu_4N^+) salt. The water-soluble Me_4N^+ salt can be reprecipitated from hot, unbuffered, pH 4.6 water to yield 15.4 g (75% yield) of product.

The elemental analyses on both the Me_4N^+ and Bu_4N^+ salts required the formulation of a six-cation system, that is, $[(Me_4N)_6H_xP_2W_{15}Nb_3O_y]_n$, where y is set at 60.5 + $x/2$ by charge balance for H^+, P^{5+}, W^{6+}, and Nb^{5+}. The absolute percentages from the elemental analysis, especially the % W (±0.6%), also require that y = 62 ± ca. 5. The IR of the product, which is very similar to the IR of $P_2W_{18}O_{62}^{6-}$, except for a 665 cm^{-1} band, strongly suggests a Dawson-like structure with y = 62. Possible formulations, then, become $[(Me_4N)_6H_{3-x}P_2W_{15}Nb_3O_{62-(x/2)}]_n$ where x = 0, n = 1 for the monomer $(Me_4N)_6H_3P_2W_{15}Nb_3O_{62}$ and x = 1, n = 2 for the single Nb–O–Nb bridged $(Me_4N)_{12}H_4P_4W_{30}Nb_6O_{123}$. Charge balance by protons is required since analysis showed none of the other possible cations, namely, Na^+ or K^+.

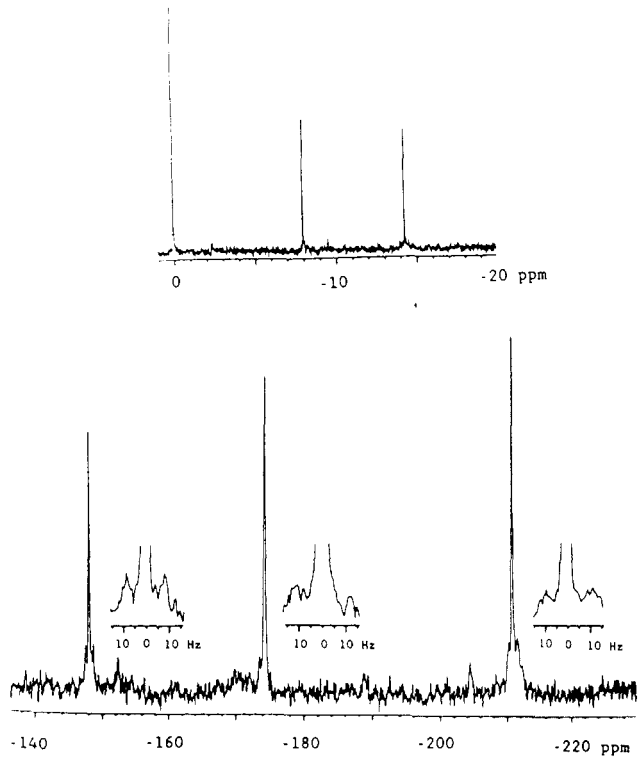

Figure 6. ^{31}P NMR spectrum (top, the 0 ppm signal is the 85% H_3PO_4 reference) and ^{183}W NMR spectrum of $Li_xH_{9-x}P_2W_{15}Nb_3O_{62}$ in D_2O. The $^2J_{W\text{-}O\text{-}W}$ couplings, which are marginally resolvable in this case, are shown as insets.

Further characterization of the protonated, *monomeric*, C_{3v} symmetry and isomerically pure α-$H_xP_2W_{15}Nb_3O_{62}^{(9-x)-}$ ($x > 0$) form in *aqueous solution* was possible by ^{31}P NMR, by solution molecular weight measurements, and by ^{183}W NMR. The high S/N ^{31}P NMR spectrum of $H_xP_2W_{15}Nb_3O_{62}^{(9-x)-}$ in unbuffered D_2O, pD 4.8, seen in Figure 6 and obtained from its soluble Li^+ and H^+ mixed-salt $Li_{9-x}H_xP_2W_{15}Nb_3O_{62}$ (from metathesis of $(Me_4N)_xH_{9-x}P_2W_{15}Nb_3O_{62}$ with $LiClO_4$ and removal of the insoluble Me_4NClO_4 by centrifugation), *is more useful in this case, and in general, than elemental analysis as a criterion of homogeneity.* Only two peaks at −8.0 and −12.4 (± 0.2) ppm are observed, establishing the level of purity for the product at >98%. Solution molecular weight measurements indicate that the $Li_{9-x}H_xP_2W_{15}Nb_3O_{62}$ salt is monomeric in unbuffered water (pH 4.6) with an observed molecular weight value of ca. 3800 (Table I, Experimental Section) which is within 8% of the calculated value of 4090 for $P_2W_{15}Nb_3O_{62}^{9-}$ (Figure B, supplementary material). It is clear then that $H_xP_2W_{15}Nb_3O_{62}^{(9-x)-}$ exists as a monomer under the slightly acidic, aqueous solution conditions used to obtain the above molecular weight.

Figure 6 illustrates the ^{183}W NMR spectrum of $Li_{9-x}H_xP_2W_{15}Nb_3O_{62}$ in D_2O (pD 4.8). The ^{183}W NMR spectrum exhibits three lines of 1:2:2 intensity at −148.0, −174.3, and −210.8 (±0.1) ppm, confirming the C_{3v} symmetry anticipated for this molecule. The −148.0 ppm peak has intensity one and can be unambiguously assigned to the three "cap" tungsten atoms (labeled **a** in Figure 3A) for $P_2W_{15}Nb_3O_{62}^{9-}$. It shows the expected large $^2J_{W\text{-}O\text{-}W}$ value (16.9 ± 1.2 Hz) due to coupling[1a-c] with the six belt tungsten atoms (labeled **b** in Figure 3A). The line at −210.8 (±0.1) ppm can be assigned to the tungstens labeled b on the basis of its two sets of $^2J_{W\text{-}O\text{-}W}$ = 17.2 and 21.3 (±1.2) Hz. The remaining peak at −174.3 ppm can then be assigned to the six belt tungsten centers, labeled **c** in Figure

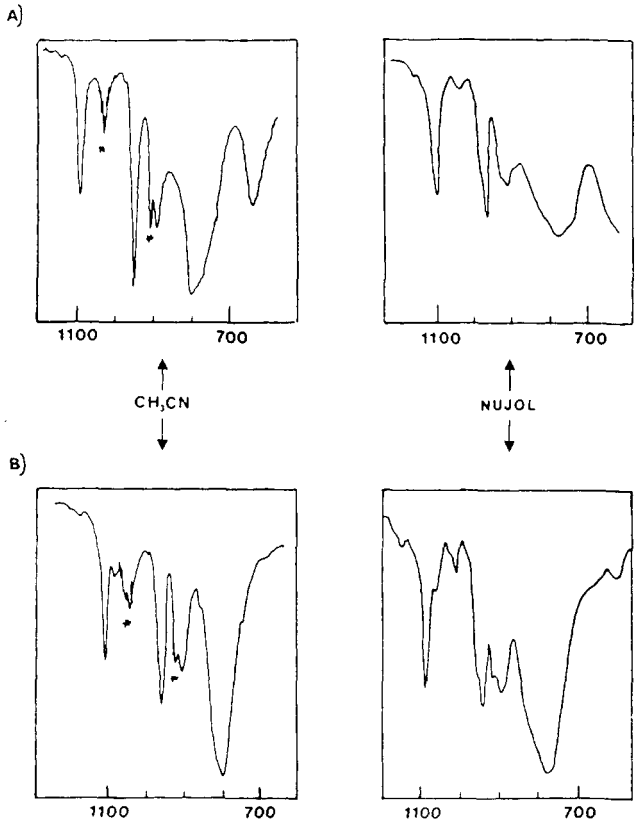

Figure 7. Infrared spectra (as acetonitrile solutions (left) and Nujol mulls (right)) of (A) $(Bu_4N)_{12}H_4P_4W_{30}Nb_6O_{123}$ and (B) $(Bu_4N)_9P_2W_{15}Nb_3O_{62}$. Solvent peaks are denoted by an asterisk.

3A, nearest to the Nb_3 cap, an assignment verified by the reciprocal $^2J_{W\text{-}O\text{-}W}$ = 23.4 (±1.2) Hz seen for both this and the −210.8 ppm resonance. The ^{183}W and ^{31}P NMR results require that a single isomer of $P_2W_{15}Nb_3O_{62}^{9-}$ has been prepared, most likely α-$P_2W_{15}Nb_3O_{62}^{9-}$,[23] on the basis of the isomerically pure α-$P_2W_{18}O_{62}^{6-}$ (and, therefore, probably α-$P_2W_{15}O_{56}^{12-}$) used in the present synthesis.

To summarize, the combination of analytical, solution molecular weight, IR, and ^{31}P and ^{183}W NMR data unequivocally establish that the previously unknown, C_{3v} symmetry $P_2W_{15}Nb_3O_{62}^{9-}$ has been prepared and that it exists as monomeric $H_xP_2W_{15}Nb_3O_{62}^{(9-x)-}$ in aqueous, pH 4.6 solution.

Since the primary focus of this work is the preparation and characterization of organic solvent-soluble heteropolyanions upon which organometallic species could be supported, much of our effort has focused upon the Bu_4N^+ salts of $P_2W_{15}Nb_3O_{62}^{9-}$. Metathesis of the Me_4N^+ with Bu_4NBr in hot, pH 4.6 unbuffered water followed by thorough washing of the resultant precipitate with hot water provided $(Bu_4N)_{12}H_4P_4W_{30}Nb_6O_{123}$ in quantitative yield on a 15-g scale. Elemental analyses for C, H, N, P, Nb, and W were within ≤±0.28% for each element. Attempts at recrystallization/reprecipitation provided inferior material (by elemental analysis; see the Experimental Section). For this reason further manipulations were avoided.

Several types of experiments were directed at determining whether the product was a monomer, a Nb–O–Nb bridged aggregate, or possibly a mixture of the two depending upon the exact conditions (e.g. pH, presence of

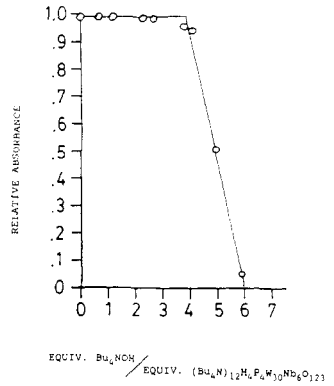

Figure 8. Spectrophotometric titration of $(Bu_4N)_{12}H_4P_4W_{30}Nb_6O_{123}$ with aqueous Bu_4NOH. The intensity of the 665 cm^{-1} IR band (attributed to a single, bridging Nb–O–Nb) is plotted vs equivalents of added base. The first 4 equiv of Bu_4NOH deprotonate the $H_4P_4W_{30}Nb_6O_{123}^{12-}$ while the last 2 equiv cleave the single Nb–O–Nb bridge in $[(P_2W_{15}Nb_3O_{61})\text{-}O\text{-}(P_2W_{15}Nb_3O_{61})]^{16-}$.

H_2O, or excess Bu_4N^+, eq 2). The IR[24] (as acetonitrile or acetone solution or Nujol mull) of what proved to be $(Bu_4N)_{12}H_4P_4W_{30}Nb_6O_{123}$ shows a 665 cm^{-1} band not present in $P_2W_{18}O_{62}^{6-}$ (Figure 7A), a band that was at first thought to be a Nb–OH (or Nb–O(H)–Nb) vibration analogous to that observed at 660 cm^{-1} for $(Bu_4N)_{7-x}H_xSiW_9Nb_3O_{40}$. However, D_2O or D^+/D_2O shifts the 660 cm^{-1} band to lower energy (Nb–OD formation) while the 665 cm^{-1} band for $H_4P_4W_{30}Nb_6O_{123}^{12-}$ is *unchanged* (as is also observed for the 690 cm^{-1} band in $Si_2W_{18}Nb_6O_{77}^{8-}$). This result has been repeated several times. Moreover, a *side-by-side control experiment* showed the 660 cm^{-1} band of $(Bu_4N)_{7-x}H_xSiW_9Nb_3O_{40}$ was shifted by deuteriation while the 665 cm^{-1} band again remained unchanged. It seemed likely, then, that the 665 cm^{-1} band is due to a bridging Nb–O–Nb linkage in $H_4P_4W_{30}Nb_6O_{123}^{12-}$, even though the 665 cm^{-1} band is broader, less intense, and at 25 cm^{-1} lower energy than the characteristic Nb–O–Nb 690 cm^{-1} vibration for $(Bu_4N)_6H_2Si_2W_{18}Nb_6O_{77}$. The key confirming experiment turned out to be a titration of IR absorbance vs equivalents of Bu_4NOH, analogous to that observed for $(Bu_4N)_6H_2Si_2W_{18}Nb_6O_{77}$. For the singly Nb–O–Nb bridged $(Bu_4N)_{12}H_4P_4W_{30}Nb_6O_{123}$, the prediction is that no change in absorbance would be observed until 4 equiv of Bu_4NOH (per equivalent of $(Bu_4N)_{12}H_4P_4W_{30}Nb_6O_{123}$) had been added to remove the four protons. The absorbance at 665 cm^{-1} should then decrease to zero as two additional equivalents of base are added to cleave the Nb–O–Nb bridge. This prediction is confirmed with the reproducible results shown in Figure 8. The results, combined with the precedent of $(Bu_4N)_6H_2Si_2W_{18}Nb_6O_{77}$ and its 690 cm^{-1} band and titration results (Figure 5), are highly suggestive of the formation of $H_4P_4W_{30}Nb_6O_{123}^{12-}$. To the extent that the break point and intercept occurs at 4.0 (observed 3.8 ± 0.4) and 6.0 equiv (observed 6.0 ± 0.4), respectively, all (±≤10%) of the material can be formulated as $H_4P_4W_{30}Nb_6O_{123}^{12-}$ with a single Nb–O–Nb bridge. Since the *solid* Me_4N^+ salt also shows this band, we tentatively formulate the solid Me_4N^+ salt as predominantly $(Me_4N)_{12}H_4P_4W_{30}Nb_6O_{123}$.

Attempts to confirm this result by solution molecular weight measurements provided initially puzzling results, since an ultracentrifugation molecular weight measurement

(23) (a) Finke, R. G.; Droege, M. W. *Inorg. Chem.* **1983**, *22*, 1006. (b) Finke, R. G.; Droege, M. W.; Hutchinson, J. R.; Gansow, O. *J. Am. Chem. Soc.* **1981**, *103*, 1587.

(24) Rocchiccioli-Deltcheff, C.; Thouvenot, R. *Spectrosc. Lett.* **1979**, *12*, 127.

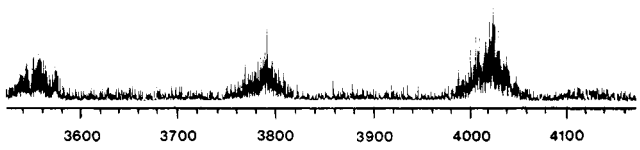

Figure 9. Negative ion FABMS (thioglycerol matrix) of $(Bu_4N)_{12}H_4P_4W_{30}Nb_6O_{123}$. The cluster centered around m/e 4026 is assigned to a $[P_2W_{15}Nb_3O_{58}]^-$ fragment as discussed in the text.

(in undried acetonitrile with the usual 0.1 M Bu_4NPF_6; Figure C, supplementary Material) gave an observed molecular weight of 4900 (Table I, Experimental Section), much closer to the $P_2W_{15}Nb_3O_{62}^{9-}$ monomer molecular weight of 4090 than to that of $P_4W_{30}Nb_6O_{123}^{16-}$, molecular weight 8165 (especially in view of the fact that we, and others, find that Bu_4N^+ salts of polyoxoanions exhibit ultracentrifugation molecular weights in acetonitrile that are systematically ca. 20% high).[13c] This experiment was repeated three times, by three of us using different samples and over a period spanning several years, with similar results, even in carefully dried acetonitrile and flame/vacuum-dried glassware. This appears to be a result of dilution and/or the presence of a large excess of Bu_4N^+ cations (see eq 2; excess Bu_4N^+ will shift this equilibrium to the left unless K_{eq} is large). This interpretation is consistent with a control experiment showing that the exact same sample, as used for ultracentrifugation, *did not show the 665 cm^{-1} band* even though this band was evident in the $(Bu_4N)_{12}H_4W_{30}Nb_6O_{123}$ sample prior to the molecular weight determination. The simplest interpretation is that, under the conditions of the ultracentrifugation solution molecular weight experiment, Nb–O–Nb cleavage to the monomer $H_xP_2W_{15}Nb_3O_{62}^{(9-x)-}$ occurs. Evidence suspporting this interpretation comes from the fact that H_2SO_4 addition yields a solution that now shows the 665 cm^{-1} IR band *and* gives evidence of a $2P_2W_{15}Nb_3O_{62}^{9-} + 2H^+ \rightleftharpoons H_2O + P_4W_{30}Nb_6O_{123}^{16-}$ equilibrium, since the ultracentrifugation solution molecular weight plot is curved and indicates one of the species present has MW $\geq$ 11 000 (for example, $[(Bu_4N)_xP_4W_{30}Nb_6O_{123}]^{x-16}$, where $x \geq 11$) (Table I and Figure D, supplementary material).

The negative ion FABMS (thioglycerol matrix) of $(Bu_4N)_{12}H_4P_4W_{30}Nb_6O_{123}$ (Figure 9) fails to detect the Nb–O–Nb bridged product. The most intense envelope (an envelope due, primarily, to the five isotopes of tungsten[5b]) occurs at m/e 4026 which corresponds to $[P_2W_{15}Nb_3O_{58}]^-$, and is probably a result of formation and dehydration of the acid anion $[H_8P_2W_{15}Nb_3O_{62}]^-$ in the FAB matrix (eq 6). Subsequent loss of WO_3 fragments results

$$[H_8P_2W_{15}Nb_3O_{62}]^- \rightarrow [4H_2O] + [P_2W_{15}Nb_3O_{58}]^- \quad (6)$$

in the peaks clustered at m/e 3794 and 3562. No parent ion for $(Bu_4N)_{12}H_4W_{30}Nb_6O_{123}$ or for $(Bu_4N)_6H_3P_2W_{15}Nb_3O_{62}$ is observed. Attempts to obtain a FABMS of a sample of the authentic deprotonated monomer $(Bu_4N)_9P_2W_{15}Nb_3O_{62}$ (thioglycerol matrix) yielded such low S/N that no fragmentation pattern could be discerned. However, Klemperer has observed that authentic $Nb_2W_4O_{19}^{4-}$ and authentic Nb–O–Nb bridged $Nb_4W_8O_{37}^{6-}$ cannot be distinguished by FABMS.[10] Consequently, it is reasonable to expect the FABMS of $(Bu_4N)_9P_2W_{15}Nb_3O_{62}$ to be very similar to that of $(Bu_4N)_{12}H_4W_{30}Nb_6O_{123}$, illustrating an important limitation of the FABMS technique as applied to such bridged polyoxoanions, a limitation first noted by Professor Klemperer.[10]

Because of our prior experience with $(Bu_4N)_4H_3SiW_9V_3O_{40}$[1c] indicating that partially protonated, mixed H^+/Bu_4N^+ salts in *dry* CD_3CN generally give low-symmetry, multiline, broadened ^{183}W and ^{51}V NMR, we were not surprised to find a several line ^{31}P NMR spectrum and broadened, poor S/N ^{183}W NMR spectrum (even after 75 000 pulses, Figure E, supplementary material) for $(Bu_4N)_{12}H_4P_4W_{30}Nb_6O_{123}$ in dry acetonitrile. Since we have shown that better S/N spectra with fewer and sharper peaks indicating higher polyoxoanion average symmetry can be obtained for $(Bu_4N)_4H_3SiW_9V_3O_{40}$ by the addition of water or pyridine,[25] similar experiments involving water or pyridine addition were done for $(Bu_4N)_{12}H_4P_4W_{30}Nb_6O_{123}$. However, less readily interpretable results were obtained. These less informative ^{31}P NMR spectra are provided as supplementary material (Figure F). We have also examined the effect of 10 equiv of H_2SO_4 on the ^{31}P and ^{183}W NMR spectra and the IR[26] of $(Bu_4N)_{12}H_4P_4W_{30}Nb_6O_{123}$ in dry CD_3CN. The ^{31}P NMR spectrum shows primarily two sharp lines (δ −11.9 and −12.1 ± 0.2) while the ^{183}W NMR spectrum yields primarily three sharp lines (δ −111.0, −144.2, and −171.7 ± 0.1; see Figure F, supplementary material).

Although these base and acid addition experiments are less valuable than anticipated, they do indicate that $P_2W_{15}Nb_3O_{62}^{9-}$ or $P_4W_{30}Nb_6O_{123}^{16-}$ has sufficient surface oxygen charge density to bind protons. Since this protonation/deprotonation problem had already been studied in considerable detail[1b] for $(Bu_4N)_4H_3SiW_9V_3O_{40}$ and because of our interest in organometallic complexes supported on $(Bu_4N)_9P_2W_{15}Nb_3O_{62}$, we decided to proceed directly to the deprotonation/cleavage of $(Bu_4N)_{12}H_4P_4W_{30}Nb_6O_{123}$ and the characterization of the resultant product.

Cleavage and Deprotonation of $(Bu_4N)_{12}H_4P_4W_{30}Nb_6O_{123}$ and Characterization of the $(Bu_4N)_9P_2W_{15}Nb_3O_{62}$ Product. The cleavage and deprotonation of $(Bu_4N)_{12}H_4P_4W_{30}Nb_6O_{123}$ by aqueous Bu_4NOH were monitored by IR, by ^{183}W and ^{31}P NMR, and by a titration of pH (mV) vs equivalents of Bu_4NOH. The latter, in DMF, Figure 10, shows the presence of three break points at 1.8, 4.2, and 5.8 (±0.4) equiv (that is, 2, 4, and 6 equiv) of added base. Changing the solvent to acetonitrile yields inflection points only at 4 and 6 equiv of added base while a mixture of acetonitrile/water/methanol yields only one breakpoint at 6 equiv of Bu_4NOH. These data can be rationalized by postulating that the species present is Nb–O–Nb bridged $H_4P_4W_{30}Nb_6O_{123}^{12-}$ $[(H_2P_2W_{15}Nb_3O_{61})$–O–$(H_2P_2W_{15}Nb_3O_{61})]$ and that each half of the Nb–O–Nb bridged species behaves largely as an isolated and independent, diprotonated molecule.

The ^{183}W NMR spectrum of $(Bu_4N)_{12}H_4P_4W_{30}Nb_6O_{123}$ in CD_3CN also showed distinct changes with the addition of successive 0.5 equiv additions of Bu_4NOH, but sharpened to three lines only after 3.0 equiv was added. The resultant 1:2:2 intensity ^{183}W NMR spectrum with peaks at −138.8, −169.5, and −207.1 (±0.1) ppm is shown in Figure 11, with the predominantly two-line ^{31}P NMR spectrum also shown (δ −7.2 and −13.8 ± 0.2). The small (≤5%) impurity peaks are possible due to $P_2W_{16}Nb_2O_{62}^{8-}$. The satellites (in the ^{183}W NMR spectrum) from which the $^2J_{W-O-W}$ values were determined are shown as insets beside

(25) Rapko, B. M. Ph.D. Dissertation, University of Oregon, June 1986.

(26) The IR spectrum of this same solution diluted with dry CH_3CN shows the 665 cm^{-1} band, indicating that the Nb–O–Nb bridge has been maintained and suggesting that H_2SO_4 induces the anticipated rapid H^+ scrambling process in $H_4P_4W_{30}Nb_6O_{123}^{12-}$. The NMR data suggest that either the ^{183}W NMR is insensitive to the C_s symmetry of this ion or that some other fluxional process is occurring.

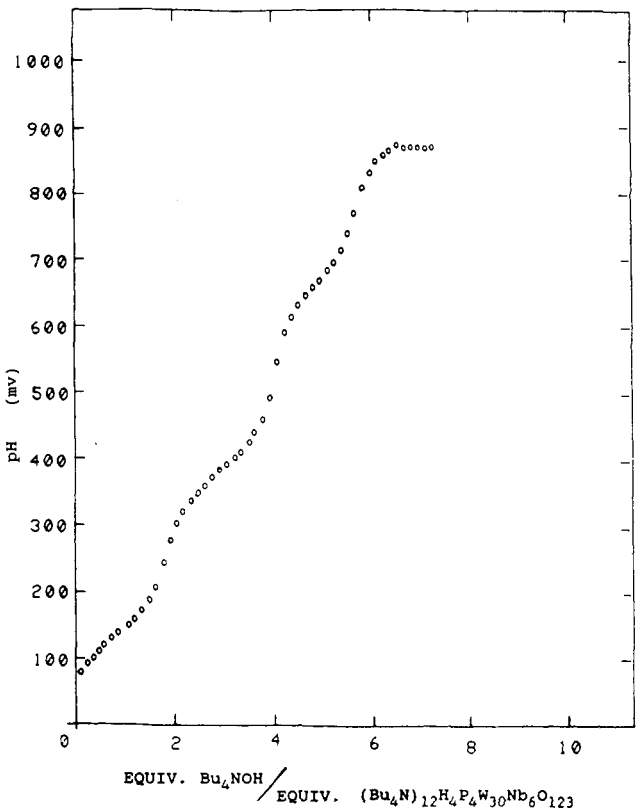

Figure 10. Millivolt titration (in DMF) of $(Bu_4N)_{12}H_4P_4W_{30}Nb_6O_{123}$ with aqueous Bu_4NOH. Breakpoints are observed at 2, 4, and 6 equiv (within experimental error) of Bu_4NOH, consistent with the presence of $[(H_2P_2W_{15}Nb_3O_{61})\text{-}O\text{-}(H_2P_2W_{15}Nb_3O_{61})]^{12-}$ as discussed in the text.

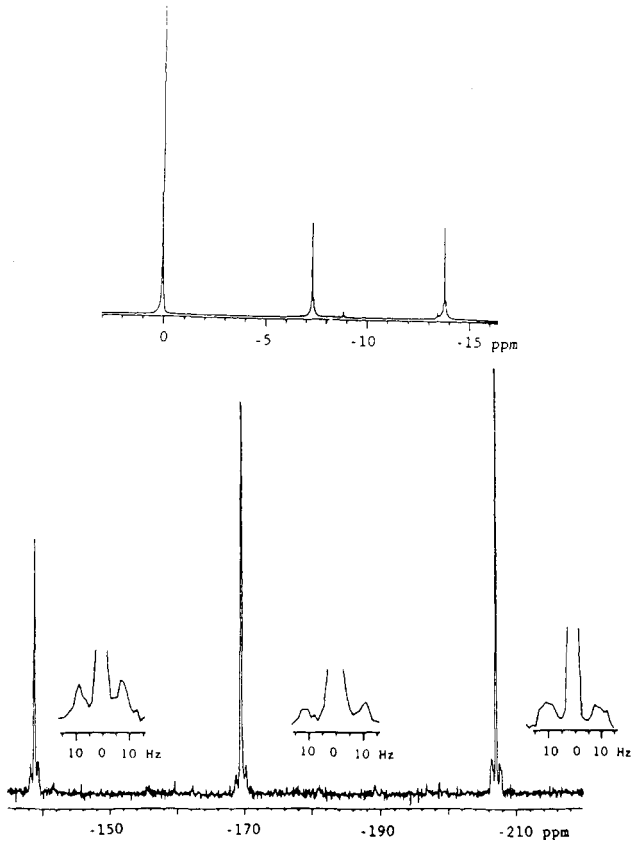

Figure 11. ^{31}P NMR spectrum (top) and ^{183}W NMR spectrum (bottom) of $(Bu_4N)_9P_2W_{15}Nb_3O_{62}$ in CD_3CN. Enlargements showing the $^2J_{W\text{-}O\text{-}W}$ satellites are shown as insets. The large resonance in the ^{31}P NMR spectrum at 0 ppm is the 85% H_3PO_4 reference.

each ^{183}W NMR peak. The −138.8 ppm resonance has intensity one and can be unambiguously assigned to the three tungsten atoms labeled **a** in Figure 3A. The assignment of the −169.5 and −207.1 ppm peaks to the six **c** and six **b** type belt tungstens, respectively (Figure 3A), follows unambiguously from the reciprocal $^2J_{W\text{-}O\text{-}W}$ as was done for $Li_{9-x}H_xP_2W_{15}Nb_3O_{62}$. The $^2J_{W\text{-}O\text{-}W}$ values do not change (compared to the $^2J_{W\text{-}O\text{-}W}$ values for $Li_xH_{9-x}P_2W_{15}Nb_3O_{62}$, within experimental error) upon deprotonation (17.1 and 22.3 (±1.2) Hz for $Li_xH_{9-x}P_2W_{15}Nb_3O_{62}$ vs 16.3 and 23.5 (±1.2) Hz for $(Bu_4N)_9P_2W_{15}Nb_3O_{62}$), suggesting, unfortunately, that $^2J_{W\text{-}O\text{-}W}$ values for $P_2W_{15}Nb_3O_{62}^{9-}$ will be relatively insensitive to supported organometallics such as $(C_5Me_5)Rh^{2+}$ and $(C_6H_6)Ru^{2+}$.

The solution molecular weight measurement of monomeric $(Bu_4N)_9P_2W_{15}Nb_3O_{62}$ in acetonitrile (Table I, Experimental Section, and Figure H, supplementary material) yielded a value of 4800 ± 400, consistent with a monomeric formulation as shown. The IR of $(Bu_4N)_9P_2W_{15}Nb_3O_{62}$ in both acetonitrile and as a Nujol mull are shown in comparison to those for $(Bu_4N)_{12}H_4P_4W_{30}Nb_6O_{123}$ in Figure 7. The disappearance of the 665 cm^{-1} band (attributed to a bridging Nb–O–Nb vibration) is evident as is an increase in intensity of the 800 cm^{-1} band (assigned to an intratriad M–O–M stretch[24]).

Synthesis and Solution Spectroscopic Characterization of the Supported Organometallic Complexes $[(C_5Me_5)Rh\cdot P_2W_{15}Nb_3O_{62}]^{7-}$ and $[(C_6H_6)Ru\cdot P_2W_{15}Nb_3O_{62}]^{7-}$. Our studies of organometallic derivatives supported on $P_2W_{15}Nb_3O_{62}^{9-}$ began with robust complexes such as $(C_5Me_5)Rh^{2+}$ which, following attachment to the polyoxoanion, would be relatively inert and protected from further chemistry by the C_5Me_5 ligand and which could be compared to $[(C_5Me_5)Rh\cdot SiW_9Nb_3O_{40}]^{5-}$ (Figure 2B).[1a] We also have examined $(C_6H_6)Ru^{2+}$, which has not been previously supported on a polyoxoanion and have studies in progress of complexes with more labile ligands that are catalyst precursors, notably, $Ir(COD)^+$ (COD = 1,5-cyclooctadiene).

In the case of $(C_5Me_5)Rh^{2+}$, refluxing of an orange-yellow acetonitrile solution of $[Rh(C_5Me_5)(CH_3CN)_3](BF_4)_2$ with a colorless acetonitrile solution of $(Bu_4N)_9P_2W_{15}Nb_3O_{62}$ resulted in a red-orange solid (after removal of the solvent under vacuum for 24 h at room temperature). All attempts to crystallize the crude product have failed, presumably due to the presence of >6 Bu_4N^+ cations, so that the product currently contains 2 equiv of Bu_4NBF_4. Solution molecular weight measurements in acetonitrile for $(Bu_4N)_7[(C_5Me_5)Rh\cdot P_2W_{15}Nb_3O_{62}]$ yielded an experimentally observed value of 5400 ± 400 or ca. 25% greater than the calculated value[13d] of 4328 for the isolated anion $[(C_5Me_5)Rh\cdot P_2W_{15}Nb_3O_{62}]^{7-}$ (Table I, Experimental Section, and Figure I, supplementary material), establishing that the product is monomeric in solution as expected.

Criteria for homogeneity can be found in the ^1H and ^{31}P NMR spectra, with a single resonance for the C_5Me_5 group seen in the high field, high S/N 360-MHz ^1H NMR spectrum at 1.92 (±0.005) ppm in CD_3CN, and two major peaks seen in the ^{31}P NMR spectrum at −8.1 and −13.8 (±0.2) ppm (Figure 12). No resonances are observed in the ^1H NMR spectrum at 1.86 ppm, indicating the absence of free $[Rh(C_5Me_5)(CH_3CN)_3]^{2+}$. The smaller peaks in the ^{31}P NMR spectrum are due to impurities of unknown composition and are estimated to be <5% of the total product.

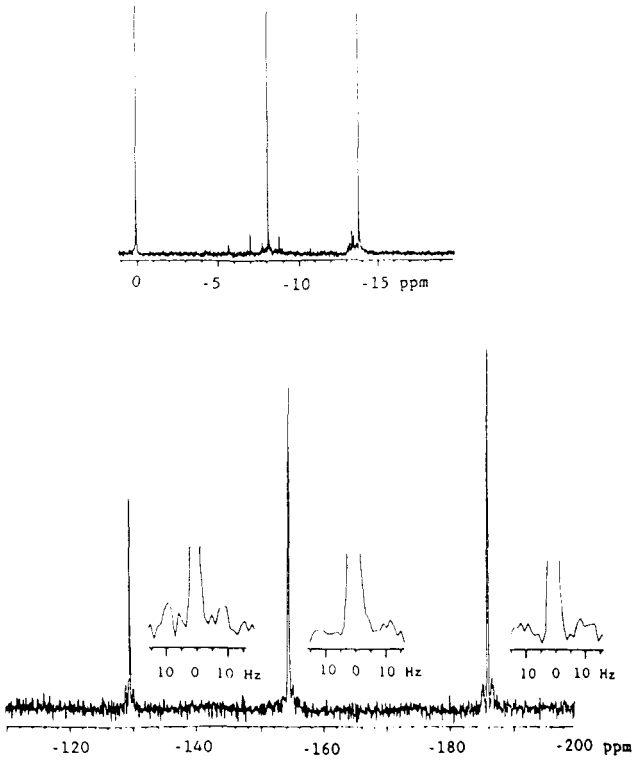

Figure 12. ^{31}P NMR spectrum (top) and ^{183}W NMR spectrum (bottom) of $(Bu_4N)_7[(C_5Me_5)Rh{\cdot}P_2W_{15}Nb_3O_{62}]$ in CD_3CN. Insets (bottom spectrum) show the $^2J_{W\text{-}O\text{-}W}$ satellites.

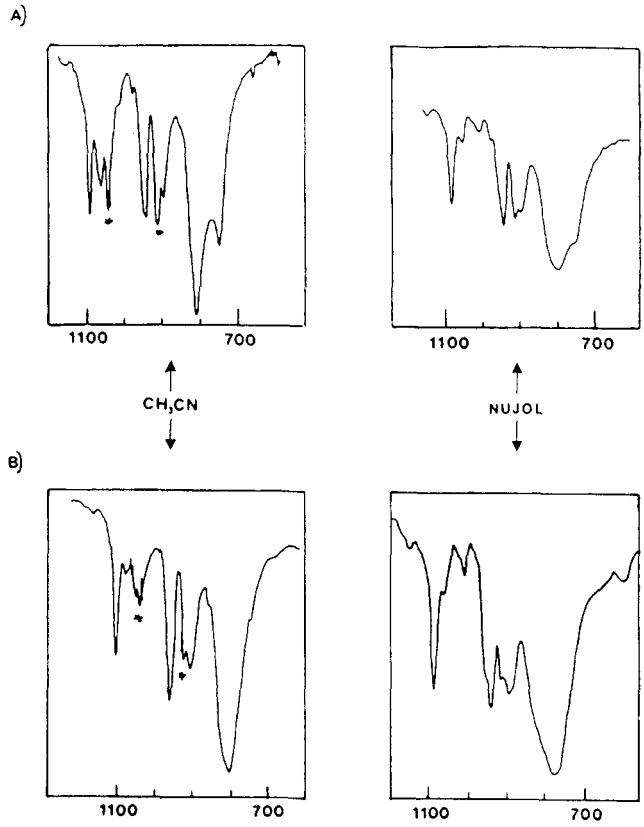

Figure 13. Infrared spectra (in acetonitrile solutions (left) and Nujol mulls (right)) of (A) $(Bu_4N)_7[(C_5Me_5)Rh{\cdot}P_2W_{15}Nb_3O_{62}]$ and (B) $(Bu_4N)_9P_2W_{15}Nb_3O_{62}$. Solvent absorbances are indicated by an asterisk.

Evidence for the covalent, inner-sphere bonding of $(C_5Me_5)Rh^{2+}$ to $P_2W_{15}Nb_3O_{62}^{9-}$ is provided by numerous physical characterizations, including ion-exchange experiments, IR, ^1H and ^{31}P NMR (vide supra), ^{183}W NMR, and the lack of other ligands (i.e. CH_3CN) for $(C_5Me_5)Rh^{2+}$.

To show that an inner-sphere, supported complex [rather than an $(C_5Me_5)Rh(CH_3CN)_3^{2+}$ ion-paired complex] had formed, an acetonitrile solution of $(Bu_4N)_7[(C_5Me_5)Rh{\cdot}P_2W_{15}Nb_3O_{62}]$ was loaded onto a cation-exchange column in the Bu_4N^+ form (Ⓟ-$SO_3^-Bu_4N^+$, Ⓟ = macroreticular polymer), and the solution slowly eluted down the column. As expected, the colored, polyanionic, $(C_5Me_5)Rh{\cdot}P_2W_{15}Nb_3O_{62}^{7-}$ complex passed down the column unchanged as determined by ^1H, ^{31}P, and ^{183}W NMR, affirming the overall anionic charge. As a control experiment, $[Rh(C_5Me_5)(CH_3CN)_3](BF_4)_2$ was dissolved in acetonitrile and loaded onto the same column. As expected, elution was not effective in removing the cationic, colored $[Rh(C_5Me_5)(CH_3CN)_3](BF_4)_2$ from the top of the resin column. Conversely, when an acetonitrile solution of $[Rh(C_5Me_5)(CH_3CN)_3](BF_4)_2$ is loaded onto an anion-exchange column in the Cl^- form (Ⓟ-$NR_3^+Cl^-$), it passes down the column with the slowly moving solvent front, whereas all of the colored, polyanionic $[(C_5Me_5)Rh{\cdot}P_2W_{15}Nb_3O_{62}]^{7-}$ is retained at the top of the resin. Even by themselves, these simple ion-exchange (or nonexchange) experiments provide good evidence for inner-sphere $(C_5Me_5)Rh^{2+}$ to $P_2W_{15}Nb_3O_{62}^{9-}$ bonding.

A comparison of the IR spectra of $(Bu_4N)_9P_2W_{15}Nb_3O_{62}$ and $(Bu_4N)_7[(C_5Me_5)Rh{\cdot}P_2W_{15}Nb_3O_{62}]$ (Figure 13), both as acetonitrile solutions and Nujol mulls, reveals that only one significant change has resulted upon support of $(C_5Me_5)Rh^{2+}$ on the heteropolyanion. The 800 cm^{-1} band in the spectrum of $(Bu_4N)_7[(C_5Me_5)Rh{\cdot}P_2W_{15}Nb_3O_{62}]$, which is assigned to intratriad M–O–M stretching vibrations,[24] now has a pronounced shoulder at 740 cm^{-1} (as if the 800 cm^{-1} band has "split" by 60–65 cm^{-1}). A similar shoulder (corresponding to a 60 cm^{-1} splitting") is seen in the IR of $(Bu_4N)_8[(OC)_3Re{\cdot}P_2W_{15}V_3O_{62}]$.[25] This shoulder at 740 cm^{-1} was also observed in acetone and Nujol mull, ruling out the possibility that it is derived from the solvent. A splitting of an analogous band has been previously seen in the IR of $(Bu_4N)_5[(C_5Me_5)Rh{\cdot}SiW_9Nb_3O_{40}]$ (by 30 cm^{-1})[1a] and $(Bu_4N)_4[(C_5H_5)Ti{\cdot}SiW_9V_3O_{40}]$ (by 35 cm^{-1}).[1c] Further examination of the IR spectrum of $(Bu_4N)_7[(C_5Me_5)Rh{\cdot}P_2W_{15}Nb_3O_{62}]$ as a KBr disk or Nujol mull reveals a lack of bands corresponding to coordinated CH_3CN. The only plausible inner-sphere ligands for $(C_5Me_5)Rh^{2+}$, then, are the surface oxygens of $P_2W_{15}Nb_3O_{62}^{9-}$.

The changes in the ^{31}P NMR peak positions for $(Bu_4N)_7[(C_5Me_5)Rh{\cdot}P_2W_{15}Nb_3O_{62}]$ in CD_3CN (−8.1 and −13.8 (±0.2) ppm (Figure 12)) are small when compared to the peaks seen for $(Bu_4N)_9P_2W_{15}Nb_3O_{62}$ (−7.3 and −14.1 (±0.2) ppm). This is not surprising, since both the primary and secondary coordination environments around the phosphorus atoms remain unchanged. More likely would be significant changes in the ^{183}W NMR spectrum of $[(C_5Me_5)Rh{\cdot}P_2W_{15}Nb_3O_{62}]^{7-}$ and this is indeed the case. Figure 12 illustrates the ^{183}W NMR spectrum of $(Bu_4N)_7[(C_5Me_5)Rh{\cdot}P_2W_{15}Nb_3O_{62}]$ in CD_3CN, with $^2J_{W\text{-}O\text{-}W}$ seen as insets. The three-line spectrum demonstrates the overall C_{3v} symmetry of the complex on the ^{183}W NMR time scale.

Two comparisons to the ^{183}W NMR spectrum of $(Bu_4N)_9P_2W_{15}Nb_3O_{62}$ need to be made. First, the peak positions in the spectrum of $(Bu_4N)_7[(C_5Me_5)Rh{\cdot}P_2W_{15}Nb_3O_{62}]$ have all shifted downfield to −128.9, −152.6, and −185.2 (±0.1) ppm, each by a significant but different amount from the corresponding peaks at −138.8, −169.5, and −207.1 (±0.1) ppm in the spectrum of $(Bu_4N)_9P_2W_{15}Nb_3O_{62}$. Second, the $^2J_{W\text{-}O\text{-}W}$ for each peak

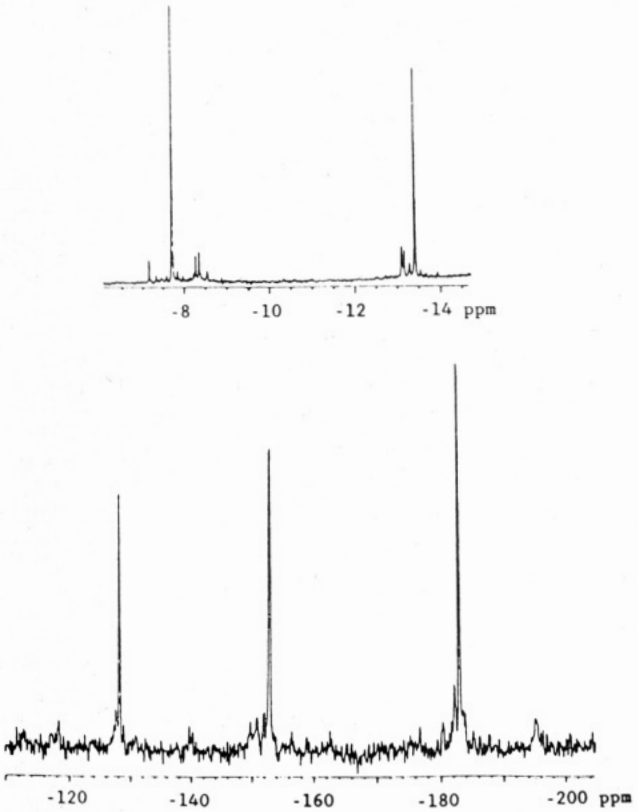

Figure 14. ^{31}P NMR spectrum (top) and ^{183}W NMR spectrum (bottom) of $(Bu_4N)_7[(C_6H_6)Ru{\cdot}P_2W_{15}Nb_3O_{62}]$ in CD_3CN.

verifies that the peak assignments made earlier for $(Bu_4N)_9P_2W_{15}Nb_3O_{62}$ and $Li_{9-x}H_xP_2W_{15}Nb_3O_{62}$ also apply to $(Bu_4N)_7[(C_5Me_5)Rh{\cdot}P_2W_{15}Nb_3O_{62}]$, and that the magnitude of these coupling constants, 18.1 and 24.6 (±1.2) Hz, are not greatly different (as expected) from those seen for $(Bu_4N)_9P_2W_{15}Nb_3O_{62}$, 15.9 and 29.5 (±1.2) Hz. This is consistent with the observed insensitivity of $^2J_{W\text{-}O\text{-}W}$ values to protonation in $(Bu_4N)_{12}H_4P_4W_{30}Nb_6O_{123}$ and can be rationalized by the support/protonation site (three NbO_6 octahedra) being four bonds removed from the W–O–W bonds involved in $^2J_{W\text{-}O\text{-}W}$ couplings (see Figure 3A).

The preparation of $(Bu_4N)_7[(C_6H_6)Ru{\cdot}P_2W_{15}Nb_3O_{62}]$ follows a procedure similar to that described above for $(Bu_4N)_7[(C_5Me_5)Rh{\cdot}P_2W_{15}Nb_3O_{62}]$. A reddish green acetonitrile solution of $[Ru(C_6H_6)(CH_3CN)_3](BF_4)_2$ was mixed with a colorless acetonitrile solution of $(Bu_4N)_9P_2W_{15}Nb_3O_{62}$. Following reflux for 1 h, a red solid is isolated after removal of the solvents under vacuum for 24 h at room temperature.

Both the ^1H and ^{31}P NMR spectra in CD_3CN of the resultant $(Bu_4N)_7[(C_6H_6)Ru{\cdot}P_2W_{15}Nb_3O_{62}]$ imply the existence of only a single species in solution. The ^1H NMR spectrum exhibits only one resonance at 5.97 (±0.005) ppm assigned to the C_6H_6 moiety; no peaks at 6.20 (±0.005) ppm, corresponding to $(C_6H_6)Ru^{2+}$, are observed. The ^{31}P NMR spectrum (Figure 14) shows two major peaks at −7.7 and −13.4 (±0.2) ppm, along with some smaller peaks, which establishes that predominantly one heteropolyanion species is present in solution.

Ion-exchange experiments similar to those performed on $[(C_5Me_5)Rh{\cdot}P_2W_{15}Nb_3O_{62}]^{7-}$ were done with $[(C_6H_6)Ru{\cdot}P_2W_{15}Nb_3O_{62}]^{7-}$ and yielded identical results. The complex $[Ru(C_6H_6)(CH_3CN)_3](BF_4)_2$ was retained on a cation-exchange resin (in the Bu_4N^+ form) while $(Bu_4N)_7[(C_6H_6)Ru{\cdot}P_2W_{15}Nb_3O_{62}]$ passed through unaltered. The latter compound was also retained at the top of an anion-exchange column (in the Cl^- form) while a control showed that $[Ru(C_6H_6)(CH_3CN)_3](BF_4)_2$ passed down the column unaffected. Each experiment was monitored by ^1H and ^{31}P NMR.

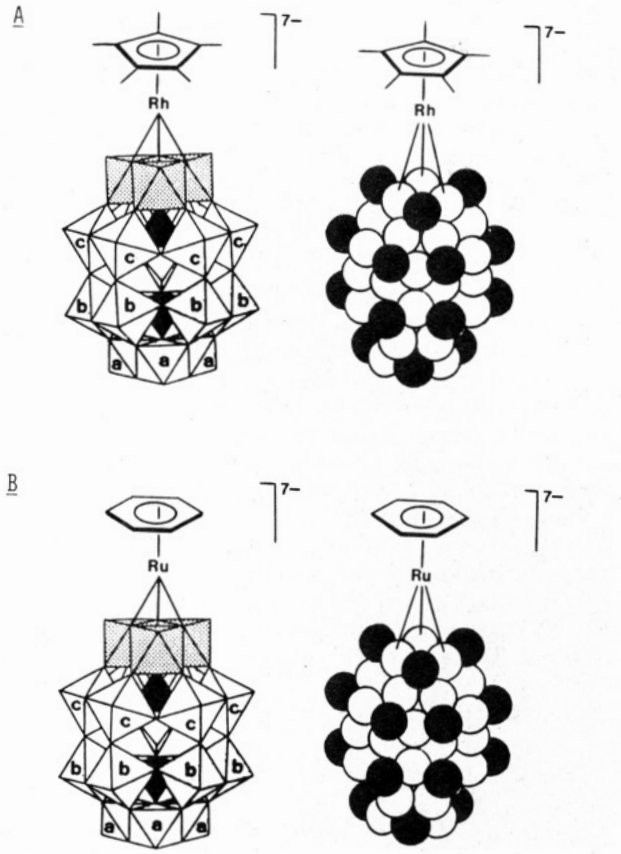

Figure 15. Structures for (A) $(C_5Me_5)Rh{\cdot}P_2W_{15}Nb_3O_{62}^{7-}$ and (B) $(C_6H_6)Ru{\cdot}P_2W_{15}Nb_3O_{62}^{7-}$ of overall (average) C_{3v} symmetry (on the NMR time scale) based on the ^{31}P and ^{183}W NMR data provided in the text. Both coordination polyhedra (left) and space-filling (right) representations for the polyoxoanions are shown. The massive $P_2W_{15}Nb_3O_{62}^{9-}$ polyoxoanion is the largest soluble oxide support system developed to date and is unusual and important in that it provides predominantly a single regioisomer of the supported organometallic.

The IR spectrum of $(Bu_4N)_7[(C_6H_6)Ru{\cdot}P_2W_{15}Nb_3O_{62}]$ in acetonitrile is similar to that obtained for $(Bu_4N)_7[(C_5Me_5)Rh{\cdot}P_2W_{15}Nb_3O_{62}]$. No absorbances due to coordinated acetonitrile are observed, which again supports the formation of a covalent, inner-sphere $[(C_6H_6)Ru{\cdot}P_2W_{15}Nb_3O_{62}]^{7-}$ species.

The ^{183}W NMR spectrum of $(Bu_4N)_7[(C_6H_6)Ru{\cdot}P_2W_{15}Nb_3O_{62}]$ in CD_3CN (Figure 14) shows three peaks at −128.2, −152.9, and −183.0 (±0.1) ppm, again indicating a species of overall C_{3v} symmetry. $^2J_{W\text{-}O\text{-}W}$ could not be seen for any of these peaks, even after prolonged data acquisition times, so peak assignments cannot be verified. However, since this complex exhibits the same C_{3v} symmetry and the same overall charge as $[(C_5Me_5)Rh{\cdot}P_2W_{15}Nb_3O_{62}]^{7-}$, it is logical to suspect that the peak assignments are the same as those discussed earlier for $P_2W_{15}Nb_3O_{62}^{9-}$ and $[(C_5Me_5)Rh{\cdot}P_2W_{15}Nb_3O_{62}]^{7-}$.

Figure 15 shows C_{3v} symmetry structures for the polyoxoanion-supported $(C_5Me)Rh^{2+}$ and $(C_6H_6)Ru^{2+}$ that are consistent with, and fully supported by, the spectroscopic data cited. The species in Figure 15 are noteworthy in two respects: they are the largest, most massive soluble oxide support materials to date, and they yield, by design, single regioisomers when supporting organometallic cations.

Summary and Conclusions

The polyoxoanion $P_2W_{15}Nb_3O_{62}^{9-}$ was designed to provide three adjacent, B-type, edge-sharing NbO_6 octahedra as a C_{3v} symmetry site for support of organometallic moieties and, eventually, for catalytic studies. Work in this paper describes the synthesis and characterization of the previously unknown $H_4P_4W_{30}Nb_6O_{123}^{12-}$ as its Me_4N^+ salt or its organic-solvent-soluble Bu_4N^+ salt. In addition, deprotonation/cleavage of $(Bu_4N)_{12}H_4P_4W_{30}Nb_6O_{123}$ to $(Bu_4N)_9P_2W_{15}Nb_3O_{62}$ without decomposition has been demonstrated. Furthermore, two inner-sphere, regiospecifically attached, and covalently bonded organometallic derivatives, $(Bu_4N)_7[(C_5Me_5)Rh{\cdot}P_2W_{15}Nb_3O_{62}]$ and $(Bu_4N)_7[(C_6H_6)Ru{-}P_2W_{15}Nb_3O_{62}]$, have been synthesized and characterized in solution by a variety of spectroscopic techniques. These derivatives have C_{3v} symmetry. Efforts at the nontrivial task of producing crystalline salts of them for X-ray diffraction structural analysis are continuing.[8a,b]

Other studies with the $P_2W_{15}Nb_3O_{62}^{9-}$ polyoxoanion-support systems are in progress, notably the isolation and characterization of the catalyst precursor $\{(COD)Ir{\cdot}P_2W_{15}Nb_3O_{62}^{8-}\}_x$ and hydrogenolysis of its coordinated 1,5-COD to produce an interesting polyoxoanion-supported catalyst. These and other studies will be reported in due course.

Acknowledgment. Support from NSF Grant CHE-8313459 is gratefully acknowledge.

Registry No. $K_7HNb_6O_{19}$, 92762-45-3; Nb_2O_5, 1313-96-8; KOH, 1310-58-3; $Na_{12}P_2W_{15}O_{56}$, 84750-84-5; α-$K_6P_2W_{18}O_{62}$, 93240-37-0; $Na_{12}P_2W_{15}O_{56}{\cdot}18H_2O$, 114714-81-7; $(Me_4N)_{12}H_4P_4W_{30}Nb_6O_{123}$, 114594-66-0; $(Bu_4N)_{12}H_4P_4W_{30}Nb_6O_{123}$, 114594-65-9; $(Bu_4N)_9P_2W_{15}Nb_3O_{62}$, 114691-26-8; $(DBU{\cdot}H)_9P_2W_{15}Nb_3O_{62}{\cdot}11H_2O$, 114672-71-8; $(Bu_4N)_7[(C_5Me_5)Rh{\cdot}P_2W_{15}Nb_3O_{62}]$, 114594-64-8; $[Rh(C_5Me_5)Cl_2]_2$, 12354-85-7; $(Bu_4N)_7[(C_6H_6)Ru{\cdot}P_2W_{15}Nb_3O_{62}]$, 114594-63-7; $[Ru(C_6H_6)Cl_2]_2$, 37366-09-9; ^{183}W, 14265-81-7.

Supplementary Material Available: Spectrophotometric titration of $(Bu_4N)_{12}H_4P_4W_{30}Nb_6O_{123}$ with aqueous Bu_4NOH while the IR absorbances were monitored at 665, 800, 905, and 955 cm^{-1} (Figure A); plot of ln A vs r^2 (from ultracentrifugation molecular weight determinations) for $Li_{9-x}H_xP_2W_{15}Nb_3O_{62}$ (Figure B), for $(Bu_4N)_{12}H_4P_4W_{30}Nb_6O_{123}$ (Figure C), for the $P_2W_{15}Nb_3O_{62}^{9-} \rightleftharpoons 2H_2O + P_4W_{30}Nb_6O_{123}^{16-}$ equilibrium formed when H_2SO_4 is added (Figure D), for $(Bu_4N)_9P_2W_{15}Nb_3O_{62}$ (Figure H), and for $(Bu_4N)_7[(C_5Me_5)Rh{\cdot}P_2W_{15}Nb_3O_{62}]$ (Figure I); ^{183}W NMR spectrum and ^{31}P NMR spectrum (inset) of $(Bu_4N)_{12}H_4P_4W_{30}Nb_6O_{123}$ in dry acetonitrile (Figure E); successive ^{31}P NMR spectra of a dry acetonitrile solution $(Bu_4N)_{12}H_4P_4W_{30}Nb_6O_{123}$ after addition of 0–4 equiv of pyridine (Figure F); and ^{183}W and ^{31}P NMR spectra of $(Bu_4N)_{12}H_4P_4W_{30}Nb_6O_{123}$ plus 10 equiv H_2SO_4 in dry CD_3CN (Figure G) (9 pages). Ordering information is given on any current masthead page.

Mechanism of the Conversion of Intermediate 16-Electron Tungstenocene Alkyls into Alkene Hydrides and Fluxionality within $[W(\eta\text{-}C_5H_5)_2(CH_2{=}CHCH_3)H]PF_6$

John P. McNally[1a] and N. John Cooper*[,1,2]

Departments of Chemistry, Harvard University, Cambridge, Massachusetts 02138, and University of Pittsburgh, Pittsburgh, Pennsylvania 15260

Received June 16, 1987

$[W(\eta\text{-}C_5H_5)_2(\text{propene})H,D]^+$ (1^+-d_n) has been prepared from $[W(\eta\text{-}C_5H_5)_2Cl_2]$ and $(CD_3)_2CHMgBr$ to determine whether β-elimination within 16-electron tungstenocene alkyls can occur by an α-elimination/1,2-hydride shift mechanism. The complex isotopic distribution within the product arises from a combination of intermolecular exchanges during the workup and intramolecular scrambling reactions. Protonation of $[W(\eta\text{-}C_5H_5)_2(CD_2{=}CDCD_3)]$ has been used to monitor the latter. Spin population transfer (spt) studies have established magnetization transfer from the hydride into the propene methyne in 1^+-endo and into the methylene in 1^+-exo, consistent with rapid reversible insertion of the propene into the W–H bond in both isomers. E_a for insertion in 1^+-endo is 24.4 (7) kcal mol^{-1} with $\Delta H^\ddagger$ = 23.7 (7) kcal mol^{-1} and $\Delta S^\ddagger$ = 11.5 (1.8) eu (k_1 = 0.694 (18) s^{-1} at 79 °C). Insertion in 1^+-exo proceeds at ca. $^1/_6$ this rate with k_1 = 0.112 (25) s^{-1} at 79 °C. The absence of spt from the hydride into the exo methyl of 1^+-exo indicates that the methyl groups in the isopropyl intermediate do not exchange on the spt time scale, probably as a result of an agostic interaction between the methyl group formed in the insertion and the unsaturated metal center. Difference spt experiments on 1^+-endo indicate that reversible α-elimination/1,2-hydride shift processes, if they occur, must have a rate <2% of the observed insertion/β-elimination process. Photolysis of $[W(\eta\text{-}C_5H_5)_2(CH_2CH_2CH_3)(NCCH_3)]PF_6$ led to exclusive formation of 1^+-endo (>99%) and free CH_3CN, indicating that transient $[W(\eta\text{-}C_5H_5)_2(CH_2CH_2CH_3)]^+$ leads specifically to the isomer of 1^+ predicted by the β-elimination mechanism. Similarly, β-elimination within transient $[W(\eta\text{-}C_5H_5)_2\{CH(CH_3)_2\}]^+$, generated by chloride abstraction from $[W(\eta\text{-}C_5H_5)_2\{CH(CH_3)_2\}Cl]$, led exclusively to 1^+-exo. The interconversion of 1^+-endo and 1^+-exo, followed by ^1H NMR from both directions, occurs by a first-order reversible reaction with k_2 and k_{-2} of 0.102 (4) and 0.139 (5) h^{-1}, respectively, at 25 °C and E_a = 22.4 (0.4) kcal/mol, $\Delta H^\ddagger$ = 21.8 (0.4) kcal/mol, and $\Delta S^\ddagger$ = −2.4 (1.2) eu for the conversion of 1^+-endo to 1^+-exo. The isomerization is suggested to involve alkene rotation.

Introduction

Coordinatively unsaturated transition-metal alkyls are typically unstable and may undergo α-, β-, or γ-elimination reactions to generate alkylidene, alkene, or metallocyclic ligands respectively.[3] β-Elimination is much the best established of these processes,[4] and it is generally accepted

(1) (a) Harvard University. (b) University of Pittsburgh.
(2) Address correspondence to N.J.C. at the University of Pittsburgh.

(3) (a) Kochi, J. K. *Organometallic Mechanisms & Catalysis*; Academic: New York, 1978; Chapter 12. (b) Schrock, R. R.; Parshall, G. W. *Chem. Rev.* **1976**, *76*, 243–268. (c) Davidson, P. J.; Lappert, M. F.; Pearce, R. *Chem. Rev.* **1976**, *76*, 219–242.

0276-7333/88/2307-1704$01.50/0